



Neuroprotective Mitochondrial Remodeling by AKAP121/PKA Protects HT22 Cell from Glutamate-Induced Oxidative Stress

Jingdian Zhang¹ · Jiachun Feng¹ · Di Ma¹ · Feng Wang² · Yumeng Wang³ · Chunxiao Li¹ · Xu Wang¹ · Xiang Yin¹ · Ming Zhang⁴ · Ruben K. Dagda⁵ · Ying Zhang¹

Received: 7 September 2018 / Accepted: 19 December 2018 / Published online: 16 January 2019
© Springer Science+Business Media, LLC, part of Springer Nature 2019

Abstract

Protein kinase A (PKA) is a ser/thr kinase that is critical for maintaining essential neuronal functions including mitochondrial homeostasis, bioenergetics, neuronal development, and neurotransmission. The endogenous pool of PKA is targeted to the mitochondrion by forming a complex with the mitochondrial scaffold A-kinase anchoring protein 121 (AKAP121). Enhanced PKA signaling via AKAP121 leads to PKA-mediated phosphorylation of the fission modulator Drp1, leading to enhanced mitochondrial networks and thereby blocking apoptosis against different toxic insults. In this study, we show for the first time that AKAP121/PKA confers neuroprotection in an in vitro model of oxidative stress induced by exposure to excess glutamate. Unexpectedly, treating mouse hippocampal progenitor neuronal HT22 cells with an acute dose or chronic exposure of glutamate robustly elevates PKA signaling, a beneficial compensatory response that is phenocopied in HT22 cells conditioned to thrive in the presence of excess glutamate but not in parental HT22 cells. Secondly, redirecting the endogenous pool of PKA by transiently transfecting AKAP121 or transfecting a constitutively active mutant of PKA targeted to the mitochondrion (OMM-PKA) or of an isoform of AKAP121 that lacks the KH and Tudor domains (S-AKAP84) are sufficient to significantly block cell death induced by glutamate toxicity but not in an oxygen deprivation/reperfusion model. Conversely, transient transfection of HT22 neuronal cells with a PKA-binding-deficient mutant of AKAP121 is unable to protect against oxidative stress induced by glutamate toxicity suggesting that the catalytic activity of PKA is required for AKAP121's protective effects. Mechanistically, AKAP121 promotes neuroprotection by enhancing PKA-mediated

Electronic supplementary material The online version of this article (<https://doi.org/10.1007/s12035-018-1464-3>) contains supplementary material, which is available to authorized users.

✉ Ying Zhang
zhang_ying99@jlu.edu.cn

Jingdian Zhang
1552978848@qq.com

Jiachun Feng
fengjcfank@qq.com

Di Ma
madi2017@jlu.edu.cn

Feng Wang
fengwang@jlu.edu.cn

Yumeng Wang
yumeng15@mails.jlu.edu.cn

Chunxiao Li
licx15@mails.jlu.edu.cn

Xu Wang
wangxu7014@mails.jlu.edu.cn

Xiang Yin
doc_yinxiang2015@163.com

Ming Zhang
zhangming99@jlu.edu.cn

Ruben K. Dagda
rdagda@medicine.nevada.edu

¹ Department of Neurology and Neuroscience Center, First Hospital of Jilin University, Xinmin Street No. 71, Changchun 130000, China

² National-Local Joint Engineering Laboratory of Animal Models for Human Diseases, Changchun, Jilin, China

³ Department of Physiology, College of Basic Medical Sciences, Norman Bethune Health Science Center, Jilin University, Xinmin Street No. 126, Changchun 130000, China

⁴ Department of Pharmacology, College of Basic Medical Sciences, Jilin University, 126 Xin Min Street, Changchun 130021, Jilin, China

⁵ Department of Pharmacology, Reno School of Medicine, University of Nevada, Mailstop 318, Howard Medical Sciences Building 148A (Office), Reno, NV 89557, USA

phosphorylation of Drp1 to increase mitochondrial fusion, elevates ATP levels, and elicits an increase in the levels of antioxidants GSH and superoxide dismutase 2 leading to a reduction in the level of mitochondrial superoxide. Overall, our data supports AKAP121/PKA as a new molecular target that confers neuroprotection against glutamate toxicity by phosphorylating Drp1, to stabilize mitochondrial networks and mitochondrial function and to elicit antioxidant responses.

Keywords Protein kinase A · A-kinase anchoring protein 121 · Dynamin-related protein 1 (Drp1) · Oxidative stress · HT22 · Mitochondrion

Abbreviations

SOD2	Superoxide dismutase 2
t-GSH	Total glutathione
AKAP121	A-kinase anchor protein 121
cAMP	Cyclic adenosine monophosphate
CREB	cAMP response element-binding protein
Drp1	Dynamin-related protein 1
D-AKAP1	Dual specificity A-kinase anchoring protein 1

Background

Glutamate, an endogenous excitatory neurotransmitter that binds to ionotropic receptors, is utilized by approximately one third of all synapses in the central nervous system to propagate action potentials [1]. However, when used at a high concentration, glutamate can be detrimental to neuronal survival. Indeed, glutamate-induced neuronal death contributes to the development and pathology of neurodegenerative diseases including Parkinson's disease (PD) and Alzheimer's disease (AD) [1, 2]. The pathological mechanisms that contribute to glutamate-mediated toxicity have been very well characterized over the past two decades. For instance, in neurons, glutamate excitotoxicity involves the overt activation of ionotropic glutamate receptors by glutamate which leads to a transient increase in Ca^{2+} fluxes, a disruption in calcium homeostasis, an elevation in detrimental levels of reactive oxygen species (ROS), the activation of the mitochondrial permeability transition pore, mitochondrial dysfunction/swelling, and the induction of secondary excitotoxicity which ultimately leads to neurodegeneration [3]. Recently, a second mechanism of neurodegeneration induced by glutamate toxicity was identified not to involve the binding of glutamate to ionotropic glutamate receptors. Indeed, it has been reported that high concentrations of extracellular glutamate blocks glutamate/cysteine antiporters which inhibits cysteine uptake and leads to an imbalance of the levels of cysteine, a reduction in cellular glutathione levels, and a detrimental accumulation of excess ROS derived mainly from mitochondria [4–6]. This second type of glutamate toxicity is known as glutamate oxidative toxicity.

HT22 cells, an immortalized mouse hippocampal progenitor cell line which lacks ionotropic glutamate receptors in its undifferentiated state, is an excellent *in vitro* model for

unveiling the molecular mechanisms of neurodegeneration induced by a variety of toxic insults that elicit oxidative stress. Indeed, the depletion of the antioxidant glutathione promotes cell death via the overt activation of the cysteine/glutamate antiporter caused by exposure to excess glutamate and by elevating the level of reactive oxygen species (ROS), leading to mitochondrial dysfunction and activation of apoptosis. The HT22 cell line can undergo glutamate-mediated cell death via a pathological pathway that does not involve the activation of ionotropic glutamate receptors [4, 6, 7]. Hence, by using the HT22 hippocampal mouse cell line, several studies have unveiled the neuroprotective potential of the antioxidant superoxide dismutase 2 (SOD2) for blocking glutamate-mediated oxidative stress and cell death in HT22 neuronal cells [6].

Mitochondria, the main generators of ATP and the predominant source of intracellular ROS, are highly dynamic organelles that exhibit bidirectional mobility and can undergo mitochondrial fragmentation (fission) or increased interconnectivity (fusion). Mitochondrial fission and fusion (MFF) are catalyzed by large mitochondrial GTPases of the dynamin superfamily to alter the shape and interconnectivity of mitochondria which ultimately govern critical cellular functions including cell survival, cellular bioenergetics, Ca^{2+} buffering, free radical homeostasis, mitochondrial DNA inheritance, and mitochondrial quality control [8]. For instance, mitochondrial fission is an early molecular event that is required for initiating apoptosis, whereas inhibiting fission can block or delay apoptosis in a variety of cell types including neurons [9–11]. Secondly, mitochondrial remodeling, mediated by the MFF machinery, governs cell survival against variety of environmental stressors including high doses of glutamate in neurons [12].

Dual specificity A-kinase anchoring protein 1 (D-AKAP1)—known as AKAP140/149 and other splice variants AKAP121 (mouse homolog of human AKAP1) and the shorter splice variant S-AKAP84 lacking Tudor and KH domains—is a protein scaffold of PKA that binds to type II regulatory subunits (RII) to target the catalytic subunit of PKA (PKA/C) to the outer mitochondrial membrane (OMM). Therefore, increasing the level of the PKA/C to the OMM leads to an increase in PKA-mediated phosphorylation of the pro-apoptotic protein BAD and of the pro-fission protein Drp1 [13–15]. For the purposes of this study, the protein complex formed by association of AKAP121 with the regulatory and

catalytic subunits of PKA (AKAP121/PKA) is also known as mitochondrial PKA [16]. In neurons, enhanced PKA-mediated phosphorylation of human Drp1 in serine 637 (serine 656 in rat Drp1) leads to enhanced mitochondrial fusion, stabilizes mitochondrial networks, increases mitochondrial health, suppresses autophagy, and governs mitochondrial trafficking and content [14, 17]. The physiological consequences of enhanced PKA-mediated phosphorylation of Drp1 lead to enhanced cell survival against a myriad of toxic insults in neurons [8, 14, 16]. In addition, enhancing PKA signaling in the mitochondrion via transiently expressing AKAP121 reverses mitochondrial pathology and dysfunction in neuronal cells that are deficient for endogenous PINK1, a ser/thr kinase that is mutated in genetic forms of Parkinson's disease [16]. Additionally, AKAP121, but not S-AKAP84, harbors C-terminal domains that serve to maintain mitochondrial health. For instance, the K homology (KH) of AKAP121 is an RNA-binding motif that binds and promotes translocation of superoxide dismutase 2 (SOD2) mRNA from the cytosol to the mitochondrion, leading to an increase in the level of SOD2 to the mitochondrion [18].

In this study, we investigated the ability of endogenous mitochondrial PKA to protect HT22 neuronal cells from cell death induced by a depletion of the antioxidant glutathione as a consequence of acute exposure to excess glutamate. By employing molecular biology techniques, our data suggest that elevating endogenous levels of AKAP121 via transient overexpression techniques robustly protects HT22 hippocampal neuronal cells from glutamate oxidative toxicity. Mechanistically, AKAP121-mediated neuroprotection in a model of oxidative glutamate toxicity requires a normoxic environment and involves PKA-mediated phosphorylation of Drp1, which leads to enhanced mitochondria interconnectivity, increased mitochondrial content, enhanced mitochondrial-derived ATP levels, and an increase the levels of antioxidants SOD2 and of glutathione to buffer excessive ROS. Overall, our observations suggest that touting PKA signaling in the mitochondrion can confer neuroprotection against oxidative stress induced by acute or chronic exposure to glutamate toxicity. Secondly, this study poses mitochondrial PKA as an excellent molecular target to develop future therapies tailored for the treatment of neurodegenerative diseases that are associated with increased oxidative stress and a depletion of glutathione including PD.

Materials and Methods

Reagents

Dulbecco's modified Eagle's medium (DMEM), 10% fetal bovine serum (FBS), 0.25% trypsin-EDTA solution (containing 0.5 g/L trypsin and 0.2 g/L EDTA), Lipofectamine2000

(Fisher Scientific, Waltham, MA), and 1% 10,000 U/mL penicillin and 10 mg/streptomycin were obtained from Gibco (Invitrogen, Carlsbad, CA). The Cell Counting Kit-8 (CCK-8) was purchased from Dojindo Molecular Technologies Incorporation (Kumamoto, Japan). L-Glutamate was obtained from Sigma-Aldrich (St. Louis, MO).

Cell Culture

Parental HT22 murine hippocampal neuronal cells were generously provided by Dr. Xingshun Xu (Institute of Neuroscience, Soochow University, China). HT22 hippocampal cells were maintained in DMEM supplemented with 10% (v/v) FBS and 1% antibiotics (penicillin-streptomycin) (Invitrogen, Grand Island, NY) and maintained at 37 °C and 5% CO₂. Cells were passaged at least three times a week. To select glutamate-resistant HT22 cell clones, we seeded 6.5×10^5 cells in a T75 flask prior to exposing cells to 10 mM glutamate for 24 h. Surviving HT22 cells were then expanded and re-exposed to 20 mM glutamate, followed by two additional rounds of exposing cells to 20 mM glutamate at a reduced cell density (3×10^5 /flask). Finally, surviving HT22 cells were exposed to 20 mM glutamate for 48 h for the last of the four rounds of selections. Glutamate-resistant HT22 cells were further maintained in complete media supplemented with 10 mM glutamate. For the purposes of this study, HT22 cells that were maintained and passaged following several sequential rounds of glutamate exposure were christened as "glutamate-resistant HT22 cells" (HT22-R) [19].

Plasmids and Cell Transfection

The pEGFP-N1 vector carrying a rat homolog S-AKAP84, which lacks the KH and Tudor domains, and the pcDNA3.1 vector harboring V5/His-tagged full-length mouse AKAP121 were graciously provided by Dr. Antonio Feliciello (Department of Molecular Medicine & Medical Biotechnology, University of Naples, Naples, Italy). A plasmid harboring a DNA insert that encodes for an N-terminally GFP-tagged fusion of the catalytic subunit of PKA and containing an outer mitochondrial membrane (OMM)-targeted leader sequence from hexokinase I (amino acids 1–30) [8] was kindly provided by Dr. Steven Green (Biology Department, University of Iowa, IA, USA). For the purposes of this study, this construct is termed OMM-PKA. DNA plasmids containing inserts that encode for GFP-tagged rat Drp1-S656D in the pEGFP-N1 plasmid and that co-express single hairpin RNA (shRNA) directed against all mammalian orthologs of endogenous Drp1 [20] were kindly provided by Dr. Stefan Strack (Department of Pharmacology, University of Iowa Carver College of Medicine, IA, USA). GFP-tagged fusion constructs expressing the core domain (residues 1–524) of wild-type rat AKAP121 or a mutant form that is

deficient for binding PKA (Δ -PKA; I310P, and L316P) were sub-cloned to the pEGFP-N1 vector. These GFP-tagged constructs of AKAP121 (wild type and PKA-binding deficient) were kindly provided by Dr. Stefan Strack. A vector that contains an insert that encodes for GFP targeted to the OMM via the yeast MAS70 (yeast homolog of TOM20) in the pEGFP-N1 vector (OMM-GFP) was kindly provided by Dr. Stefan Strack and served as a control vector for all experiments that involved transfecting cells with GFP-tagged AKAP121 plasmids. The empty vector pcDNA3.1 was employed as a control vector for studies involving the transfection of HT22 cells with V5/His-tagged AKAP121.

In order to transiently transfect HT22 cells with PKA modulating plasmids, cells were seeded at a density of 1.2×10^5 cells per well in 6-well cell culture plates and transfected upon reaching confluency ($\sim 85\%$). For each well of the 6-well cell culture plate, up to 2500 ng of control plasmids and cDNAs that harbored proteins of interest, 5 μ l Lipofectamine 2000, and 250 μ l Opti-MEM were pipetted in a sterile Eppendorf tube and incubated for 20 min at room temperature. The cDNA/Lipofectamine complexes were overlaid into each well of 6-well cell culture plate seeded with HT22 cells. Twenty-four hours post-transfection, cells were harvested and lysed for total GSH, ATP, and Western blot analyses or re-seeded in 96-well plate or poly-D-lysine-coated 35 mm Nest Glass Bottom Dishes overnight to perform cell survival experiments or mitochondrial morphology and content assays as further described below.

Oxygen-Glucose Deprivation/Re-oxygenation

Ischemia was performed *in vitro* by inducing oxygen-glucose deprivation followed by re-oxygenation (OGD/R) as previously published [21]. In brief, normal, complete medium (DMEM containing FBS and glucose) was replaced with FBS/glucose-free DMEM (Gibco®) medium and hypoxia was induced by exposing cells to a gas mixture of 5% CO₂ and 95% N₂. Following a period of 3 h or 6 h oxygen-glucose deprivation (OGD) period, cells were switched to normal medium and normoxic conditions for 1 h. The Cell Counting Kit-8 (CCK-8, Dojindo Molecular Technologies Incorporation) assay was then employed to quantitate cell death normalized to control conditions as further described below (CCK-8 assay subsection).

Preparation of Whole Cell Lysates and Western Blot

For preparation of the whole cell lysates from untreated or treated cells (e.g., glutamate, dibutiryl-cyclic AMP, or transfected), cells were washed with cold PBS, then suspended in 150 μ l of RIPA lysis buffer containing 50 mM

Tris (pH 7.4), 150 mM NaCl, 1% NP-40, 0.5% sodium deoxycholate, 0.1% SDS, 1 mM EDTA, protease inhibitor cocktail, and 1% PMSF. The cell debris resulting from cell lysis was then removed by centrifuging at 12,000 $\times g$ for 5 min at 4 °C and the supernatants were collected on different microcentrifuge tubes prior to analysis of relevant protein markers by Western blot.

The protein concentration was determined by employing the BCA protein assay per manufacturer's instructions (Pierce, Rockford, IL, USA). In brief, 30 μ g equal amounts of denatured proteins were subjected to SDS-PAGE gel electrophoresis (Bio-Rad, Hercules, CA) and electrophoresed proteins within the 12% acrylamide gel were transferred onto a polyvinylidene fluoride (PVDF) membrane. The PVDF membrane was then blocked with 5% BSA in TBS buffer for 1 h, at room temperature. The PVDF membranes were then incubated with the following primary antibodies: anti-human D-AKAP1 (1:1000, (D9C5)#5203, CST), anti-catalytic subunit of PKA (1:1000, ab211265, Abcam), phosphorylated CREB (Serine133) (1:5000, ab32096, Abcam), anti-total CREB (1:1000, ab32515, Abcam), anti-VDAC (1:1000, ab15895, Abcam), anti-Drp1 (1:1000, ab184247, Abcam), anti-phospho-DRP1 (Ser637) (1:1000, E-AB21251, Elabscience), anti-SOD2 (1:1000, E-AB-14360, Elabscience), anti-GFP (1:5000, E-AB-20050, Elabscience), anti- β -actin (1:2000, TA-09, Zhongshan-Bio, Beijing, China) overnight at 4 °C. Following three washes in Tris-buffered saline containing Tween 20 (TBST), the PVDF membrane was then incubated with horseradish peroxidase (HRP)-labeled secondary antibodies (Boster, BA1054, Wuhan, China) for 2 h at room temperature in the dark. Immunodetection of proteins of interest was performed by employing the electrochemiluminescence (ECL) kit (Boster, Wuhan, China) and imaged by employing a microscopic digital imaging system (Olympus, Japan).

CCK-8 Assay

Following transfection for 24 h, HT22 cells were re-seeded at a cell density of 5×10^3 cells/well in 96-well tissue culture plates and incubated overnight in 5% CO₂ at 37 °C. Cells were then exposed to 4 mM glutamate for 24 h or subjected to OGD/R insults as described in the “Oxygen-Glucose Deprivation/Re-oxygenation” section. After treatment, we switched the medium per well with 100 μ l DMEM medium containing 10% CCK-8 and incubated for an additional 3 h. The absorbance at 450 nm was measured by using a 96-well plate reader (Bio-Rad, Hercules, CA). The viability of the cells was recorded as the percentage relative to untreated controls.

Mitochondrial Morphology and Mitochondrial Content Assay in Cell Culture

HT22 cells cultured on poly-D-lysine-coated 35 mm Nest Glass Bottom Dishes were transfected by using Lipofectamine 2000 per manufacturer's instructions and as described above ("Plasmids and Cell Transfection" section). Following exposure of cells with OGD/R or treatment with excess glutamate, mitochondria and nuclei in live HT22 cells were visualized by exposing cells with 30 nM MitoTracker™ Red CMXRos (Life Technologies) for 15 min followed by one wash with warm, no phenol red medium, and exposed with 2 µg/ml Hoechst 33342 for 15 min at 37 °C and 5% CO₂ respectively. Fluorescence images of cells were captured by employing the API Delta Vision Elite Live cell Imaging System (Applied Precision) at 60× magnification by using a Plan Apo 60×/1.42 NA oil-immersion objective and equipped with FITC/TRITC/DAPI fluorescence filters and bright-field capability. Sections of the cells of interest containing fluorescently labeled mitochondria labeled by MitoTracker Red were subjected to analysis by using the Image J software (v1.46) to make Z-projections and the Biplane Imaris software (v7.4.) to generate easy 3D reconstruction videos.

Mitochondrial interconnectivity and mitochondrial content were assessed from mitochondria in HT22 cells that were manually traced in fluorescence images by calculating the average area/perimeter ratio and the percentage of the cytosol occupied by mitochondria (mitochondrial content) respectively in glutamate-treated HT22 cells by employing the "Mitochondrial Morphology" macro (available free online on the Wiki site <http://imagejdocu.tudor.lu/>) on the Image J software (v1.46) as previously described [22].

RT-qPCR

To quantitate the mRNA level of SOD2 in HT22 cells treated with excess glutamate or vehicle control, total RNA was prepared from cytosolic and mitochondrial fractions from HT22 cells by using the TRIzol reagent (Invitrogen, Carlsbad, CA, USA) per manufacturer's instructions. Total RNA was reverse transcribed into cDNA by using the "PrimeScript® 1st strand cDNA synthesis" kit (TaKaRa, Tokyo, Japan). SYBR® Green Real-time PCR Master Mix (Sigma, USA) was used to determine the mRNA level of the gene of interest by employing the Stratagene Mx3000P qPCR system (Stratagene-Agilent). The relative mRNA levels were normalized to the housekeeping gene β -actin. Relative mRNA levels of indicated gene were analyzed using the $2^{-\Delta\Delta C_t}$ method. Paired primer sequences used for amplifying SOD2 are F:5'-CCATTTTCTGGACAAACCTGA-3' and R:5'-GACCCAAAGTCACGCTTGATA-3' and for β -actin: 5'-CCAGCCTTCCTTCTTGGGTAT-3' (forward) and 5'-TGCTGGAAGGTGGACAGTGAG-3' (reverse).

Measurement of Intracellular Cyclic AMP

HT22 cells seeded in 6-well plates were treated with 4 mM glutamate for different time points (0–5 h) when cells reached approximately 90% confluency. The competitive immunoassay kit (Nanjing Jiancheng Bioengineering Institute, China) was employed to quantitate the level of intracellular cyclic AMP (cAMP) per manufacturer's instructions. In brief, the culture medium was removed from the wells, adherent cells were washed twice in cold PBS, trypsinized, and harvested in 1 mL Eppendorf tubes containing PBS. Cells were then subjected to sequential three freeze-thaw cycles to lyse cells followed by centrifugation at 3000 rpm for 20 min to remove cell debris. The supernatant was stored at –80 °C prior to measuring the level of intracellular cAMP. The optical absorbance was measured at 450 nm by employing a microplate reader (Bio-Rad, Hercules, CA) following background correction. The absolute concentration of cAMP level assayed in each sample was calculated by employing a standard curve of increasing cAMP concentrations per the manufacturer's instructions (Nanjing Jiancheng Bioengineering Institute, China).

Mitochondrial Superoxide Assay

To determine the intracellular level of mitochondrial superoxide, glutamate or vehicle-treated transfected HT22 cells were plated in 96-well tissue culture plates and mitochondrial superoxide was visualized by exposing cells to the cell permeable, red fluorescent superoxide-sensitive dye MitoSOX (Invitrogen, Grand Island, NY), as previously described and per the manufacturer's instructions with the following minor modifications. In brief, following treatment with 4 mM glutamate for 7 h, cells were stained with MitoSOX Red (5 µM; 37 °C; 15 min). After three gentle washes with warm, phenol red-free, and 4 mM glutamate-containing medium, fluorescence (510/580 nm) was read at 8 and 10 h by employing a SynergyH1 plate reader (BioTek Instrument, Inc., Winooski, VT, USA) preloaded with the Gen 5 software. In addition, cells in those aforementioned conditions were analyzed for MitoSOX levels by fluorescence microscope.

Intracellular ATP Assay and Total GSH Assay

Mitochondrial ATP concentrations were measured by using luminometer-based assays per manufacturer's instructions (ATP Assay Kit; Beyotime Institute of Biotechnology, China) and by using a 96-well plate reader as previously described [23]. In brief, after 24 h of transfection, HT22 cells grown in 96-well plates were exposed to 4 mM glutamate for another 24 h to induce glutamate oxidative toxicity. Cells were then washed with PBS prior to lysing with lysis buffer in ice. One half of the wells containing cells were treated with the

potent mitochondrial uncoupler carbonyl cyanide-p-trifluoromethoxyphenylhydrazone (FCCP) for 45 min at 3 μM to uncouple mitochondria and to determine mitochondrially derived ATP. The luminescence readings were converted to ATP concentrations (μM) based on a 0–10- μM standard curve and normalized to protein concentration by using the Bradford assay. Finally, ATP concentration was normalized to protein concentration (μmol of ATP/ μg of protein) as previously described [23].

The total level of GSH in HT22 cells were determined using commercially available kits per manufacturer's instructions (Beyotime Institute of Biotechnology, China).

Mitochondrial Isolations

For groups that necessitated the enrichment of crude mitochondrial fractions, mitochondrial and cytoplasmic fractions were isolated by using the Mitochondria/Cytosol Fractionation Kit (C3601, Beyotime Institute of Biotechnology, China) per manufacturer's instructions. In brief, HT22 cells were cultured in NEST T175 flasks, and following Lipofectamine-mediated transfection for 24 h, cells were harvested and washed twice with ice-cold PBS. Harvested cells were then incubated in 1 or 2 ml ice-cold mitochondrial lysis buffer on ice for 10 min. Cells were gently disrupted by applying 20 strokes with a glass homogenizer and pestle on ice. The resulting homogenate was then centrifuged at $600\times g$ for 10 min at 4 $^{\circ}\text{C}$ to remove any unbroken cells. The supernatant was then collected from each sample and then centrifuged at $11,000\times g$ for 10 min at 4 $^{\circ}\text{C}$ to isolate the mitochondrial fraction (pellet) by removing the cytoplasmic fraction (supernatant). The crude mitochondrial pellet was washed several times using a washing buffer and re-centrifuged for 10 min at $11,000\times g$ to isolate the processed mitochondrial fraction. Proteins were then subjected to RNA extraction or Western blot.

Measurement of Mitochondrial Membrane Potential

Changes in mitochondrial membrane potential were estimated via the uptake of the cell permeable, red fluorescent dye rhodamine 123 which enters the mitochondria as a result of the highly negative $\Delta\psi\text{m}$. Depolarization of $\Delta\psi\text{m}$ results in a significant loss of mitochondrial retention of rhodamine 123, leading to a decrease in the intracellular fluorescence. In brief, HT22 cells were harvested and incubated with rhodamine 123 (5 μM) at 37 $^{\circ}\text{C}$ for 30 min; after which, they were washed twice with warm PBS and then subject to an ACEA flow cytometer (ACEA, USA). The mean fluorescence intensities of HT22 cells were analyzed using the FlowJov10.3 software (Tree Star Inc., OR, USA).

Statistics

Results were expressed as compiled mean \pm S.E.M. Multiple group comparisons were performed using one-way analysis of variance (ANOVA) followed by Tukey's test for post hoc analyses for experiments that involved more than two experimental conditions, or followed by using Fisher's LSD *t* test for pairwise comparisons to identify significant differences. Statistical analyses were performed by using PRISM 5.01 (GraphPad). Values of $p < 0.05$ were considered significant.

Results

Glutamate-Mediated Oxidative Stress Elicit Cyclic AMP-Dependent PKA Signaling

AKAP121 (rat homolog of human D-AKAP1) can link PKA to the outer mitochondrial membrane (OMM) to promote mitochondrial fusion by phosphorylating dynamin-related protein 1 (Drp1). Enhancing the level and activity of mitochondrial PKA can enhance mitochondrial interconnectivity as a mechanism to promote neuroprotection against a variety of toxic stimuli [8, 16]. In this study, we explored for the first time the extent to which AKAP121 protects HT22 cells from oxidative glutamate toxicity and against ischemia/reperfusion. First, in order to identify the minimum and maximum concentrations of glutamate that is toxic to HT22 cells, we treated parental HT22 cells seeded in 96-well plates with increasing concentrations of L-glutamate. By using well-validated survival assays (CCK-8), we observed that exposing HT22 cells to 4 mM L-glutamine for 24 h elicited maximum cell death, whereas a 2 mM induced modest but significant cytotoxicity (25% cell death) (Fig. 1a). While glutamate-mediated toxicity can cause neuronal death through a variety of molecular pathological mechanisms (e.g., via rapid depletion of glutathione, mitochondrial fragmentation, increased superoxide levels), several studies have reported that oxidative glutamate toxicity can increase several compensatory signaling pathways to delay neuronal death [19, 24, 25]. Given that cyclic AMP-dependent PKA signaling can be altered in response to ischemia, neurodegeneration, and other toxic insults [14, 15, 26–28], we analyzed the level of intracellular cyclic AMP (cAMP) and PKA activity in HT22 cells exposed to an LD50 dose of glutamate. Interestingly, we observed that the level of intracellular cAMP concentration rose sharply within 2 h and plateaued by 2 h of glutamate treatment (Fig. 1b). In addition, it has been reported that the level of endogenous AKAP121 is transcriptionally upregulated via the transcription factor cyclic AMP-dependent response element-binding protein (CREB) in a PKA-dependent manner in other non-neuron cell types [29, 30]. To this end, we surmised that an increase in intracellular cAMP signaling is associated with

an increase in the level of endogenous AKAP121 in HT22 cells exposed to excess concentrations of glutamate. Indeed, we observed that the endogenous level of AKAP121 increased in time-dependent manner with maximal levels achieved at 8 h of exposure to excess glutamate. Consistent with the concept that oxidative glutamate toxicity enhances PKA activity, we observed that the level of phosphorylated CREB, a substrate of PKA, is also elevated as assessed by quantifying the ratio of p-CREB to T-CREB (p-CREB/T-CREB) with maximal levels of p-CREB/T-CREB ratios achieved at 8 h but decreasing by 12 h of glutamate post-treatment of HT22 cells (Fig. 1c). Overall, these experimental observations suggest that upregulation of PKA signaling increases the level of endogenous mitochondrial PKA (AKAP121/PKA). Next, we explored the extent to which levels of AKAP121 and of p-CREB/CREB are altered in HT22 cells habituated to thrive in high levels of glutamate (HT22-R cells). As in naïve HT22 cells treated with an acute dose of excess glutamate, we observed that glutamate-resistant HT22 cell contained high protein levels of AKAP121 and p-CREB/CREB ratios (Fig. 1d). Furthermore, we observed that the accumulation of AKAP121 and the phosphorylation of CREB can be blocked by incubating cells with H89 for 24 h (Fig. S1E). Given that endogenous cyclic AMP and AKAP121 levels increase in a time-dependent manner in HT22 cells treated with excess glutamate (Fig. 1c), we surmised that elevated cyclic AMP—as a consequence to glutamate oxidative toxicity—contributes to a cAMP-mediated increase in the level of endogenous AKAP121. Indeed, Western blot analyses demonstrated a significant time-dependent increase in AKAP121 protein levels in cell lysates from HT22 cells treated with exogenous 250 μ M dbt-cAMP, with maximum levels observed at 12 h post-treatment (Fig. 1e, f). Consistent with an induction of transcription, the increase in AKAP121 levels was elicited following an increase in PKA-dependent phosphorylation of the PKA regulated transcription factor CREB (ser 133) (Fig. 1e, f). Thus far, our data demonstrate that acute or chronic treatment of neuronal HT22 cells with high concentration of glutamate elicits a compensatory PKA signaling to increase AKAP121 levels, presumably as a protective response to delay cell death induced by exposure to excess concentration of exogenous glutamate.

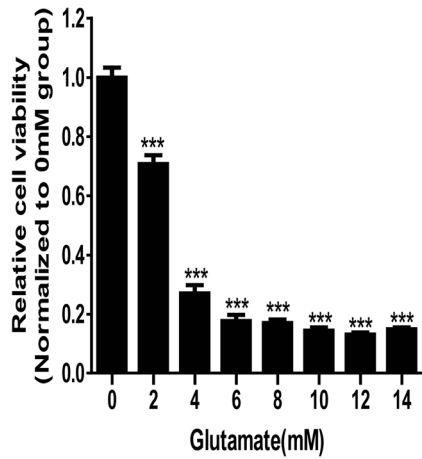
AKAP121 Overexpression Can Increase the Level of Antioxidants SOD2 and GSH as a Molecular Mechanism to Reduce Oxidative Stress

Given that the level of AKAP121 increases in a time-dependent manner in response to oxidative glutamate toxicity, we then surmised that the increased level of AKAP121 mediates the neuroprotective effects in HT22 cells in an oxidative (glutamate oxidative injury) but not in an oxygen reducing environment (hypoxia). To address this hypothesis, we

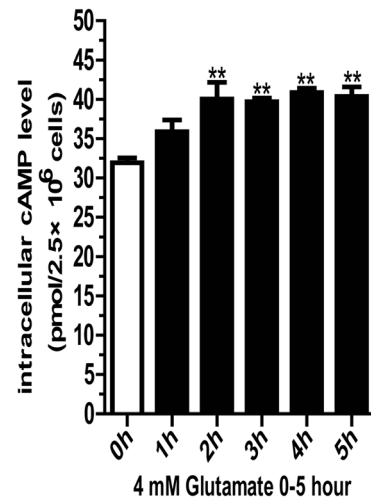
transiently overexpressed HT22 with an empty control or with full-length V5/His-tagged AKAP121 containing the KH and Tudor domains in HT22 cells (Fig. 2a) for 24 h prior to challenging them with two types of toxic insults: (1) 4 mM glutamate or (2) oxygen-glucose deprivation followed by reperfusion (OGD/R). Although exogenous full-length AKAP121 can be transiently expressed to robust levels in HT22 cells (Fig. 2b), it was unable to confer significant protection in HT22 cells subjected to ischemia/reperfusion in vitro model (Fig. 2c). In addition, given that endogenous AKAP121 is rapidly degraded via the E3 ubiquitin ligase Siah2 during OGD/R [31] and modulates levels of the mitochondrial localized antioxidant SOD2 [18], we then surmised that the level of endogenous AKAP121 is altered in cells treated with excess glutamate. However, we observed that the level of both endogenous and overexpressed AKAP121 remained unaffected in HT22 cells exposed to a high concentration of glutamate compared to untreated HT22 cells (Fig. 2b). This data is consistent with the observation that AKAP121 is degraded in an oxygen reducing environment [31] but not in an oxidative environment (Fig. 2b) and explains why AKAP121 is only able to protect against oxidative glutamate toxicity but not against OGD/R. Importantly, AKAP121-overexpressing HT22 cells show higher cell viability and an overall healthy cell morphology when treated with excess glutamate compared to vector-transfected HT22 cells as assessed by the CCK-8 assay and bright-field microscopy (Fig. 2d). Overall, this data suggest that AKAP121/PKA can protect neuronal cells against oxidative glutamate toxicity but not against OGD/R.

We then explored the mechanisms that underlie the neuroprotective effects of AKAP121 in the glutamate oxidative toxicity model. It has been reported that exposure of HT22 cells with high concentrations of extracellular glutamate blocks the glutamate/cysteine antiporter to inhibit cysteine uptake and leads to a rapid depletion of intracellular level of the antioxidant GSH in HT22 cells, an early pathological event that induces oxidative stress and rapid depletion of energy [5, 6, 24]. Consistent with these studies, we observed that both the total level of GSH (T-GSH) and intracellular ATP levels decreased sharply in HT22 cells exposed to glutamate compared to untreated cells (Fig. 2e, f). On the other hand, transient overexpression of full-length AKAP121 increased the levels of T-GSH and ATP in both untreated and in glutamate-treated cells compared to vector-transfected cells (Fig. 2g–i). Consistent with another study [5, 6], the exposure of HT22 cells to 4 mM glutamate leads to a significant increase in the level of intracellular mitochondrial-derived ROS in HT22 cells exposed to glutamate as assessed by exposing cells with the permeable, red fluorescent superoxide indicator MitoSOX Red used to analyze the level of mitochondrial superoxide [6](Fig. 2j). Given that AKAP121 increases the level of SOD2 mRNA in the mitochondria [18], we then explored the extent to which transient expression of AKAP121

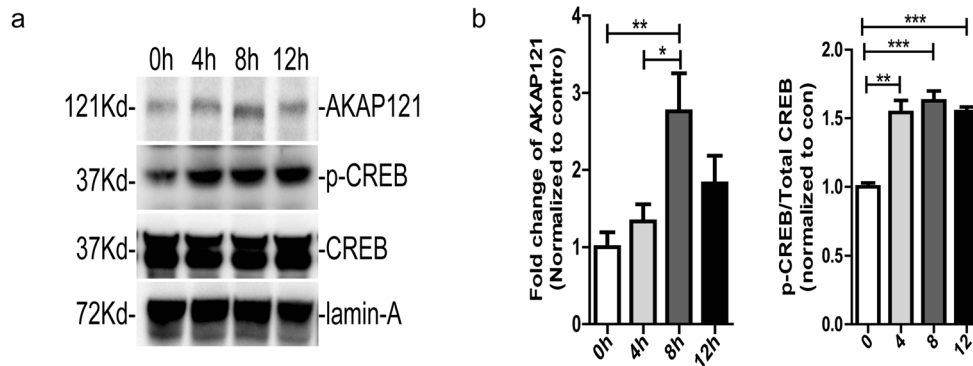
A



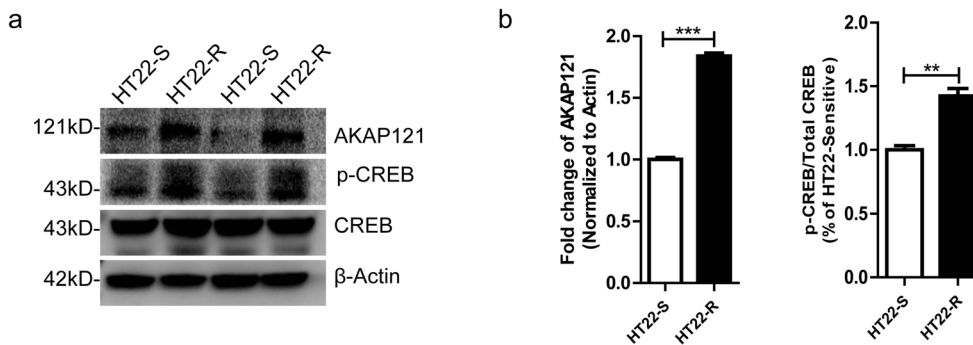
B



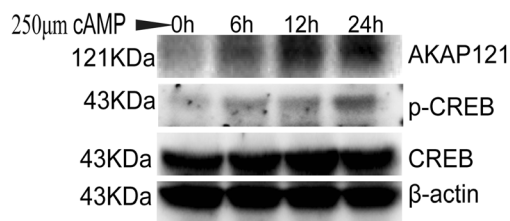
C



D



E



F

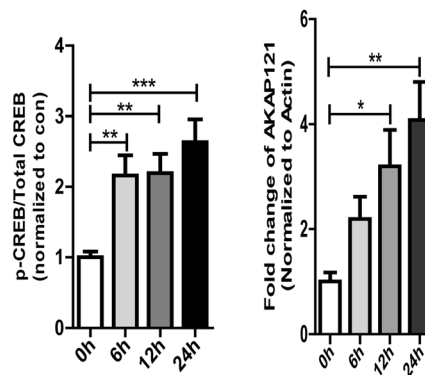


Fig. 1 Glutamate-mediated oxidative stress elicit cyclic AMP-dependent PKA signaling. **a** Effect of glutamate on cell viability. Cells were seeded in 96-well culture plates at 5000 cells/well, overnight, then treated with glutamate at the indicated concentrations for 24 h. Cell viability was determined using the CCK-8 assay ($***p < 0.001$ vs. 0 mM, one-way ANOVA, Tukey's test). **b** An intracellular rise in cAMP level is observed as a result of oxidative glutamate toxicity. Parental HT22 cells were seeded in 6-well culture plates at 2×10^5 cells per well overnight and subsequently challenged with 4 mM glutamate for the indicated time points. Cells were then harvested per well in lysis buffer and intracellular cAMP was assayed by performing the competitive immunoassay ($**p < 0.01$ vs. 0 h, one-way ANOVA, Tukey's test). **c** Cells lysates derived from parental HT22 cells that were challenged with 4 mM glutamate for the indicated time points and immunoblotted for endogenous AKAP121, p-CREB, and total CREB (T-CREB) to analyze AKAP121 level and the p-CREB to CREB ratios. The representative Western blot, representative of three experiments, (a) shows that challenging HT22 cells with glutamate increases the level of endogenous AKAP121 and of p-CREB, suggesting that glutamate toxicity is associated with increased intracellular cAMP-dependent signaling. The bar graphs on the right show densitometric-based quantifications of the mean intensity of the immunoreactive bands for AKAP121 (left bar graph) or of p-CREB/T-CREB ratio (for both graphs: $***p < 0.001$ vs. 0 h, one-way ANOVA, Tukey's test). **d** Cells lysates derived from HT22-sensitive and-resistance cell clones (HT22-R) were immunoblotted for endogenous AKAP121, p-CREB, and CREB to analyze the extent to which exposure of cells to chronic and high concentrations of glutamate elicits PKA signaling. The bar graphs on the right show image-based quantifications of the mean intensity of the immunoreactive bands for AKAP121 (left bar graph) or of p-CREB/T-CREB ratio (for both graphs: $**p < 0.01$, $***p < 0.001$ vs. HT22-S, Student's *t* test). **e** Cell lysates derived from HT22 cells incubated in 250 μ M cAMP for indicated time were immunoblotted for the level of AKAP121 and p-CREB/CREB ratio. The representative Western blot, representative of three experiments, shows that incubating HT22 cells with 250 μ M cAMP robustly increases the level of endogenous AKAP121 and of p-CREB. **f** The bar graphs show image-based quantifications of the mean intensity of the immunoreactive bands for AKAP121 (right bar graph) or of p-CREB/T-CREB ratio (left bar graph) (for both graphs: $*p < 0.05$, $**p < 0.01$, $***p < 0.001$ vs. 0 h, Student's *t* test). All the data were pooled from experiments that were repeated at least three times which yielded similar results (a representative data set is shown)

affects the levels of mitochondria-derived superoxide. We observed that transient expression of full-length AKAP121 can significantly block the increase in mitochondrial superoxide in glutamate-treated cells treated for 8 h or 10 h (Fig. 2j). Overall, our data suggests that AKAP121 promotes neuroprotection against oxidative glutamate toxicity in HT22 cells, in part by enhancing cytosolic and mitochondrial localized antioxidant defenses to reduce the level of deleterious mitochondrial superoxide.

Mitochondrial Superoxide Dismutase SOD2 Content Is Elevated in a PKA-Dependent Manner in HT22 Cells

AKAP121 possesses a K homology (KH) RNA-binding motif (Fig. 2a) that anchors SOD2 mRNA to promote its translocation to the mitochondria, leading to increased protein levels of SOD2 [18] and cytoprotection against

oxidative stress [6, 32]. Given that treatment of HT22 cells with excess glutamate is associated with a significant increase in the protein level of AKAP121 (Fig. 1c), we then surmised that an elevated protein level of AKAP121 serves to increase the mRNA and protein levels of SOD2 in the mitochondrion. To address this hypothesis, we transiently transfected HT22 cells with an empty vector or with full-length AKAP121 and analyzed for mRNA and protein levels of SOD2 by RT-qPCR and Western blot respectively. While RT-qPCR analyses showed that AKAP121-transfected HT22 cells contained a significantly lower level of SOD2 mRNA in the mitochondrial fraction compared to the untreated cells under baseline conditions (Fig. 3a, left graph), transient expression of full-length AKAP121 was associated with a significant increase in SOD2 mRNA level in cells treated with excess glutamate compared to HT22 cells transiently transfected with an empty vector as a control (Fig. 3a, right graph). Next, given that HT22-R intrinsically showed an elevated level of AKAP121 compared to naïve HT22 cells (Fig. 1d), we hypothesized that the increase in the level of AKAP121 is associated with an increase SOD2 mRNA level in order to reduce oxidative stress induced by exposure to excess glutamate. Indeed, Western blot analyses showed that HT22-R cells contained an elevated protein level of SOD2 compared to glutamate-sensitive HT22 cells (Fig. 3b). This data suggest that an increase PKA signaling and level of mitochondrial antioxidants (Figs. 1c and 3b) are compensatory mechanisms that serve to confer neuroprotection against oxidative stress in HT22-R cells. Next, we surmised that increasing the level of PKA/C at the mitochondrion is sufficient to enhance the protein level of SOD2. We observed that the protein level of SOD2 is significantly increased in cell lysates derived from HT22-R cells transfected with GFP-tagged AKAP121 (residues 1–524) compared to OMM-GFP-transfected cells (Fig. 3c). Furthermore, cell lysates derived from transient HT22-R cells transfected with a GFP-tagged PKA-binding deficient mutant of AKAP121 (residues 1–524) (AKAP121- Δ PKA) demonstrated similar level of SOD2 as HT22-R cells transfected with mitochondrial targeted GFP as a control (OMM-GFP). These data suggest that the ability of AKAP121 to bind PKA/C is required to increase the level of SOD2 at the mitochondrion (Fig. 3c). Next, we explored the extent to which increasing the catalytic activity of PKA at the mitochondrion is sufficient to increase levels of SOD2. To address this question, we transiently transfected naïve HT22 cells with a constitutively active mutant of the catalytic subunit of PKA targeted to the mitochondrion via the mitochondrial targeting sequence of hexokinase I_{1-30} and N-terminally fused to GFP (OMM-PKA) and analyzed for

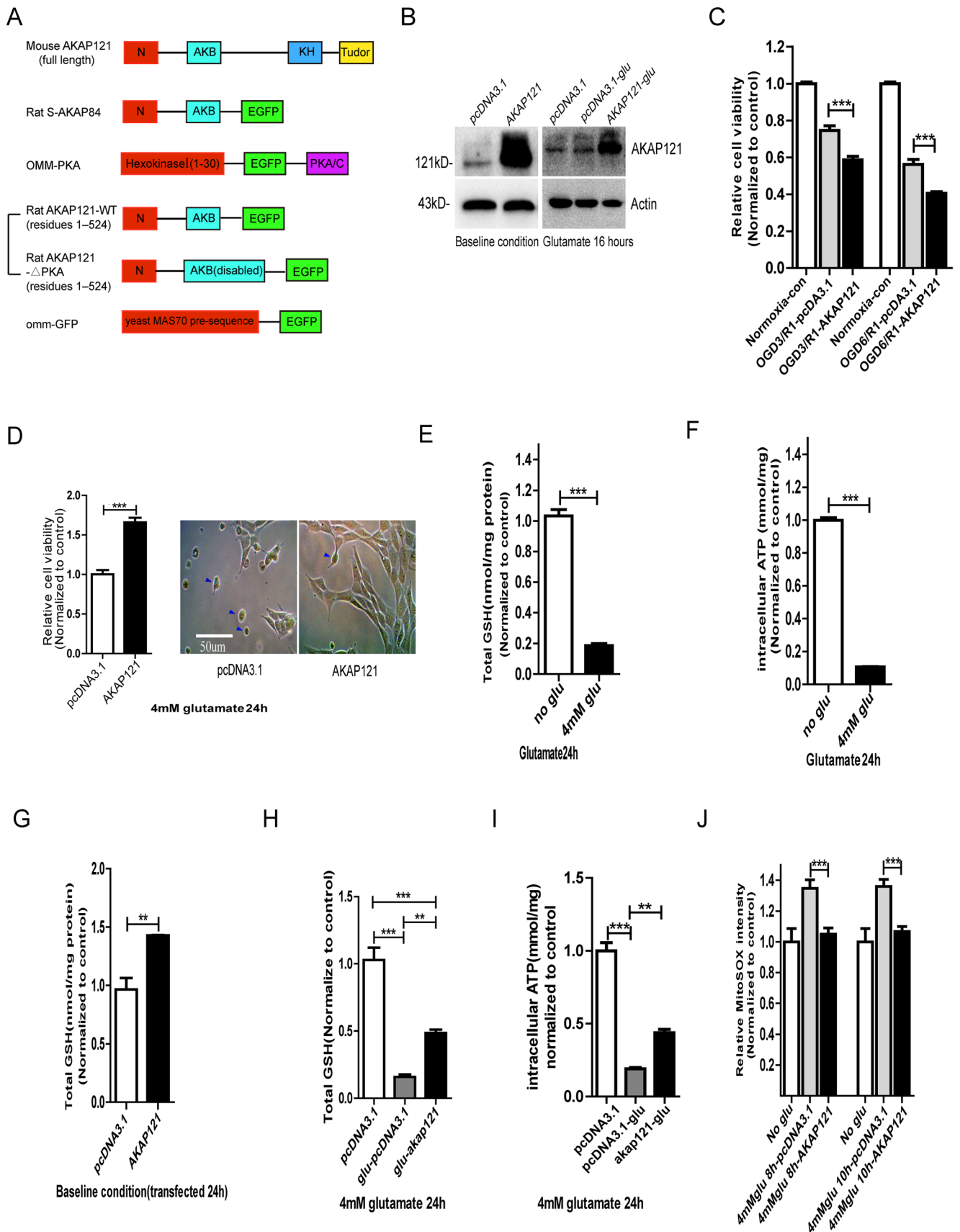


Fig. 2 AKAP121 overexpression can increase the level of antioxidants SOD2 and GSH as a molecular mechanism to reduce oxidative stress. **a** The domain structure of S-AKAP84, OMM-PKA, AKAP121, the AKAP121-WT, and AKAP121- Δ PKA pair and mitochondrial targeted GFP (OMM-GFP). The DNA constructs used in the experiments are shown in this figure and throughout Figs. 3, 4, 5, and 6. The relative positions of functional domains are labeled and indicated in different colors. “N” corresponds to the 30-residue mitochondrial targeting domain whereas the AKB stands for the PKA-binding domain of S-AKAP84, full-length AKAP121, AKAP121-WT-GFP, and AKAP121- Δ PKA-GFP. Note that the K homology (KH) and Tudor domains are homologous to the corresponding RNA-binding domains. Hexokinase I serves as the N-terminal OMM-targeting sequence for OMM-PKA. PKA/C stands for the catalytic subunit of PKA. **b** Lysates from cells transiently transfected the empty vector control (pcDNA3.1) or AKAP121 vector were immunoblotted for the level of AKAP121 under baseline conditions or in the presence of excess glutamate. **c** Cells were transfected with empty vector (pcDNA3.1) or with AKAP121 for 24 h and seeded in 96-well culture plates at 5000 cells/well overnight. Cells were then subjected with OGD/R. Cell viability was determined by employing the CCK-8 assay ($***p < 0.001$ vs. pcDNA3.1, one-way ANOVA, Tukey’s test). **d** HT22 cells were incubated with 4 mM glutamate for 24 h. The cell morphology was visualized with a phase-contrast microscope. The representative phase-contrast images show that transient expression of AKAP121 preserves normal cell morphology compared to cells expressing an empty vector ($***p < 0.001$ vs. pcDNA3.1, Student’s *t* test). Scale bar = 50 μ m. **e, f** Cell lysates derived from untreated or glutamate exposed (4 mM, 24 h) HT22 cells were assayed for the level of intracellular glutathione (**e**) and of ATP levels (**f**) (for both graphs: $***p < 0.001$ vs. no glu, Student’s *t* test). **g** Cell lysates derived from hippocampal progenitor HT22 neuronal cells transiently transfected with pcDNA3.1 empty vector control or with AKAP121 were assayed for the level of intracellular glutathione HT22 cells and normalized to protein concentration ($**p < 0.01$ vs. con-pcDNA3.1, Student’s *t* test). **h, i** Confluent HT22 cells were transfected with AKAP121 or with pcDNA3.1. Cells transfected with empty vector without glutamate incubation served as a control. 24 h post-transfection, cells were challenged with 4 mM glutamate for 24 h harvested, lysed and the intracellular total glutathione and ATP content were measured to assess the extent to which transient expression of AKAP121 restores T-GSH and ATP levels (for both graphs: $**p < 0.01$, $***p < 0.001$ vs. con-pcDNA3.1, Student’s *t* test). **j** HT22 cells were untreated or challenged with 4 mM glutamate for 8 and 10 h. Cells were then stained with the cell permeable, red fluorescent dye MitoSOX Red (5 μ M) to assess the levels of superoxide. Quantitation of fluorescence intensity of MitoSOX in HT22 cells was assessed by employing a microplate reader and normalized to cell number measured by employing the CCK-8 assay (for both 8 or 10 h exposures to glutamate: $***p < 0.001$ vs. 4 mM glut pcDNA3.1, one-way ANOVA, Tukey’s test). All the data were pooled from experiments that were repeated at least three times which yielded similar results (a representative data set is shown)

SOD2 levels by Western blot. Indeed, Western blot analyses of mitochondrial fraction derived from transiently OMM-PKA-transfected HT22 cells demonstrated significantly elevated PKA/C and SOD2 levels compared to OMM-GFP-transfected naïve HT22 cells (Fig. 3d). In aggregate, our data shows that enhanced PKA level at the mitochondrion increases the mRNA and protein levels of SOD2 in the mitochondrion, presumably as a compensatory, beneficial response to counteract oxidative stress induced by excess glutamate.

Mitochondrial Localized PKA Promotes Neuroprotection Against Glutamate Oxidative Toxicity by Remodeling Mitochondria and by Phosphorylating Drp1

Mitochondrial localized PKA phosphorylates human Drp1 in serine 637 (p-Drp1), leading to increased mitochondrial interconnectivity and enhanced neuroprotection against a variety of toxic insults and in a genetic model of PD [8, 16, 28]. S-AKAP84 is a spliced isoform of AKAP121 that lacks the KH and Tudor domains [33]. We transiently transfected naïve HT22 cells with a panel of mitochondrial PKA-modulating constructs that included the rat S-AKAP84, OMM-PKA, AKAP121-WT-GFP, and AKAP121- Δ PKA-GFP to determine whether enhancing the level and activity of mitochondrial PKA (AKAP121/PKA or S-AKAP84/PKA) confers neuroprotection against oxidative glutamate toxicity in a PKA-dependent manner in HT22 cells (Fig. 2a). It is worth noting that transient expression of all constructs (S-AKAP84, AKAP121, or OMM-PKA) can be expressed to high levels (Fig. 4a) and does not alter cell viability or cell density under basal conditions (normoxic and in complete medium) (Fig. S1A). Furthermore, epifluorescence analyses of live transfected cells demonstrated that S-AKAP84, OMM-PKA, AKAP121-WT, AKAP121- Δ PKA, and OMM-GFP are colocalized with mitochondria (Fig. 4i(c, g, k), j(c, g, k)). Next, we tested the ability of mitochondrial PKA-modulating constructs to enhance PKA activity in the mitochondrion by analyzing for the level of phosphorylated Drp1, a substrate of AKAP121/PKA and of S-AKAP84/PKA. In the absence of cAMP, Western blot analyses of cell lysates derived from HT22 cells transiently transfected with OMM-PKA resulted in an elevated ratio of p-Drp1/T-Drp1, whereas transient expression of S-AKAP84 did not significantly increase p-Drp1/T-Drp1 ratio compared to OMM-GFP-transfected cells (Fig. 4b). However, treating cells with 250 μ M cAMP for 2 h significantly elevated the ratio of p-Drp1/T-Drp1 in HT22 cells transiently expressing full-length AKAP121, S-AKAP84, and AKAP121-GFP, which lacks the KH and Tudor domains, compared to the OMM-GFP group (Fig. 4c, d). Consistent with previous studies [16], these data show that transient expression of core domain of AKAP, which is essential for binding PKA, is sufficient to enhance the rate of cyclic AMP-mediated activation of PKA in the mitochondrion. Next, we transiently overexpressed wild-type rat AKAP121 or its PKA-binding deficient mutant (AKAP121- Δ PKA) in HT22-S and HT22-R cells to further explore the importance of PKA-binding ability of AKAP121 in this model. Semi-automated morphometric analyses of mitochondria in MitoTracker-stained cells showed that transient expression of S-AKAP84, OMM-PKA, and rat AKAP121-WT, but not AKAP121- Δ PKA, induced some perinuclear clustering (Figs. 4i(e, i), j(e) and S2A-a), and elevated

mitochondrial interconnectivity and content (% of cytosol occupied by mitochondria) compared to control OMM-GFP transfected cells (Figs. 4e–h and S2B, C). In the presence of oxidative stress, HT22 cells transiently expressing AKAP121 and treated with excess glutamate show a significantly higher mitochondrial interconnectivity and content compared to cells transfected with OMM-GFP or AKAP121- Δ PKA cells and treated with glutamate for 2 h, a time point that induced a significant decrease of mitochondrial interconnectivity and content (Fig. S3A–E). Given that S-AKAP84 and AKAP121-WT-GFP lack the KH and Tudor domains, these data suggest that elevated PKA activity, but not mitochondrial

biogenesis or increased mRNA SOD2 levels, contribute to enhancing mitochondrial interconnectivity in HT22 cells in a PKA activity-dependent manner. To further corroborate whether the ability of S-AKAP84 to modulate mitochondrial interconnectivity and mitochondrial content requires PKA activity, we treated HT22 cells transiently transfected with S-AKAP84 with H89 (0.5 μ M, 4 h), a pharmacological inhibitor of PKA that does not affect baseline viability in HT22 cells (Fig. S1B, left graph). Indeed, treating HT22-transfected cells with H89 completely blocked the ability of S-AKAP84 for enhancing mitochondrial fusion and mitochondrial content per cell (Fig. S1B–D). Consistent with another study [20],

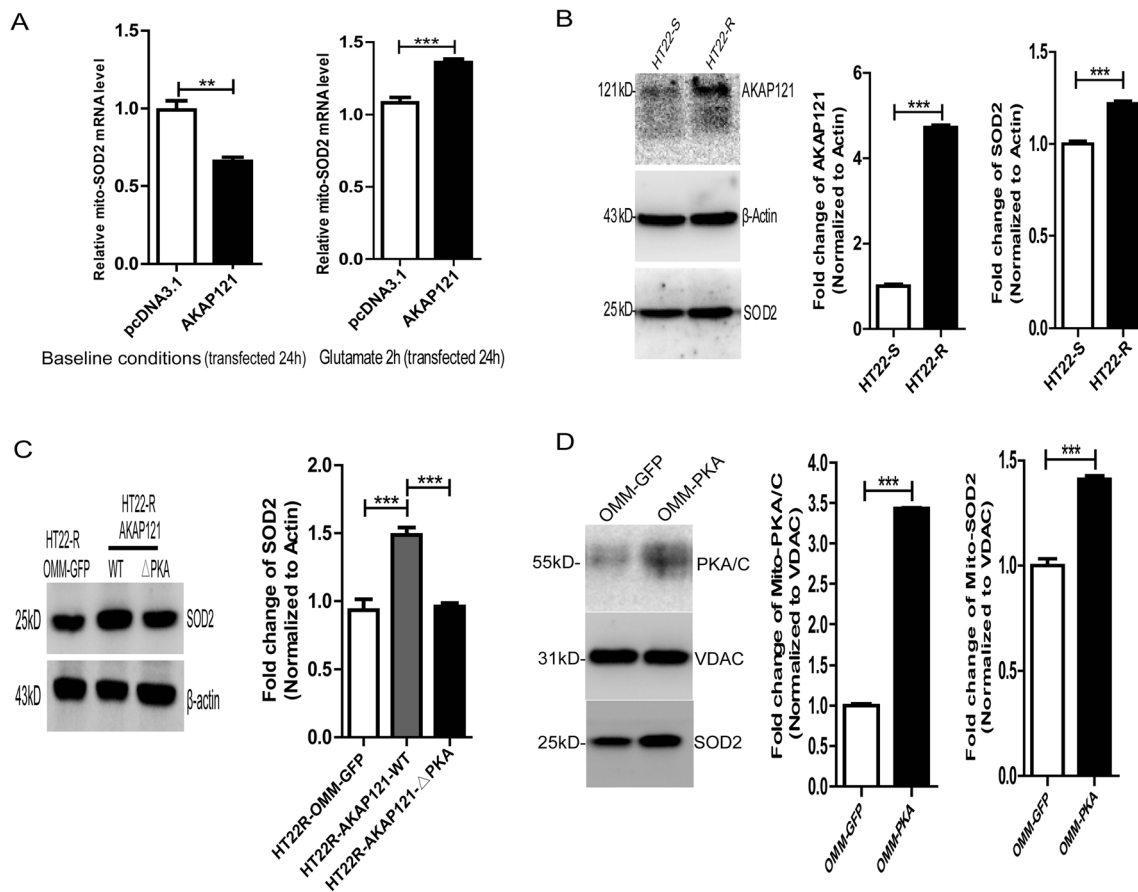


Fig. 3 Mitochondrial superoxide dismutase SOD2 content is elevated in a PKA-dependent manner in HT22 cells. **a** RT-qPCR mediated quantification of the relative mRNA level for SOD2 derived from HT22 cells transiently transfected with AKAP121 or empty control vector under baseline conditions or following treatment with excess glutamate for 2 h and normalized to β -actin. For both graphs: $**p < 0.01$, $***p < 0.001$ vs. pcDNA3.1 group, Student's *t* test). **b** Cells lysates derived from HT22-sensitive (HT22-S) or from glutamate-resistant HT22 cells (HT22-R) were immunoblotted for endogenous AKAP121, SOD2, and for β -actin as a loading control. The representative Western blot shows that HT22-R cell possesses a higher AKAP121 level together with an increasing level of SOD2 compared to HT22-S cell (for both graphs: $***p < 0.001$ vs. HT22-S, Student's *t* test). **c** Cells lysates derived from

glutamate resistant HT22 cells (HT22-R) transfected with OMM-GFP, AKAP121-WT, and AKAP121- Δ PKA were immunoblotted for endogenous SOD2 and for β -actin as a loading control ($***p < 0.001$ vs. OMM-GFP, one-way ANOVA, Tukey's test). **d** Mitochondrial fractions derived from HT22 cells transiently transfected with the indicated OMM-PKA vector were immunoblotted for PKA/C, SOD2, and VDAC as a loading control for mitochondria analyze the extent to which enhancing PKA signaling in the mitochondrion, via transient transfection of OMM-PKA, affects the protein levels of SOD2 (for both graphs: $***p < 0.001$ vs. OMM-GFP, Student's *t* test). All the data were pooled from experiments that were repeated at least three times which yielded similar results (a representative data set is shown)

our data suggest that AKAP121 enhances mitochondrial content and mitochondrial interconnectivity in a PKA activity-dependent manner in HT22 cells (Figs. 4e–h and S2B).

Mitochondrial Localized PKA Increases Total GSH, Reduces Mitochondrial ROS, and Increases Neuronal Survival

Mitochondrial dysfunction plays a critical role in the activation of programmed cell death. We then explored the extent to which increasing the activity and level of mitochondrial PKA enhances mitochondrial function and health against oxidative stress in glutamate-treated HT22 cells. Indeed, we observed that transient expression of S-AKAP84 or OMM-PKA enhanced neuronal survival against glutamate oxidative toxicity (Fig. 5a, b). Secondly, transient expression of OMM-PKA, and S-AKAP84, concomitantly increased the level of total GSH (T-GSH) content in glutamate-untreated HT22 cells (Fig. 5c). Indeed, 24 h treatment of cells with 4 mM glutamate reduced the level of total GSH in HT22-s cells (Fig. 5d). Consistent with an ability of AKAP121/PKA for enhancing mitochondrial health, transient expression of AKAP121 in HT22 cells increases the transmembrane potential of mitochondria in a PKA activity-dependent manner under baseline conditions as assessed by flow cytometry of cells stained with the potentiometric, red fluorescent dye rhodamine 123 (Fig. S4A–E). Furthermore, transient expression of AKAP121 increased the levels of mitochondrial ATP compared to HT22 cells transiently expressing OMM-GFP control (Fig. S4F). The ability of AKAP121 to increase mitochondrial ATP levels was observed to require PKA activity as treating AKAP121-expressing cells with H89 generated similar levels of ATP as in OMM-GFP expressing cells (Fig. S1D). Finally, we observed that transient expression of S-AKAP84 or OMM-PKA blocked the increase in the level of mitochondrial superoxide, as assessed by the MitoSOX assay in HT22 cells treated with glutamate for 8 and 10 h (Fig. 5f, g). Overall, our data suggest that increasing the activity of mitochondrial PKA reverses mitochondrial damage and oxidative stress induced by exposure to excess glutamate.

The Neuroprotective Effects of AKAP121 Are Conferred via PKA-Mediated Phosphorylation of Drp1

Drp1 is a *bonafide* substrate of AKAP121/PKA and PKA-mediated phosphorylation of human Drp1 in serine 637 (656 mouse homolog) inhibits mitochondria fission, leading to enhanced mitochondrial interconnectivity and cytoprotection against oxidative stress [34]. To this end, we hypothesized that the mechanism by which AKAP121 confers neuroprotection against oxidative glutamate toxicity in HT22 cells involves PKA-mediated phosphorylation of Drp1 to maintain mitochondrial interconnectivity. To

address this hypothesis, we transiently transfected HT22 cells with a plasmid that co-expresses a PKA phosphomimetic mutant of Drp1 (S656D) and shRNAs that specifically knocks down endogenous rat Drp1. This phosphomimetic mutant of Drp1 has been shown to phenocopy the neuroprotective effects of AKAP121/PKA in a genetic cell culture model of PD and in cells treated with a variety of toxic insults including rotenone and tunicamycin [16, 20]. Western blot analyses show that high levels of Drp1-S656D can be attained in transiently transfected HT22 cells by 48 h post-transfection (Fig. 6a). Semi-automated morphometric analysis of the mitochondria in transfected cells demonstrated that transient expression of Drp1-S656D enhances mitochondrial interconnectivity (area/perimeter per cell) and mitochondrial content compared to empty vector-transfected cells (Fig. 6b–d) and in a similar manner as HT22 cells transiently expressing AKAP121, S-AKAP84, or OMM-PKA under baseline conditions (Fig. 4E–H). In the presence of excess exogenous glutamate, HT22 cells transfected with Drp1-S656D or WT-AKAP121 but not AKAP121- Δ PKA completely reversed mitochondrial fragmentation and loss of mitochondrial content induced by 4 h incubation of 4 mM glutamate in OMM-GFP-transfected cells. Interestingly, transient expression of Drp1-S656D was as efficient as AKAP121 in reversing mitochondrial fragmentation and content (Fig. 6g, h). Importantly, transient transfection of Drp1-S656D significantly enhanced cell survival against glutamate-mediated toxicity relative to empty vector-transfected cells (Fig. 6f), suggesting that PKA-mediated phosphorylation of Drp1 in serine 656 via AKAP121/PKA is sufficient to enhance neuronal survival against oxidative glutamate toxicity by promoting mitochondrial interconnectivity. Finally, we then investigated whether the PKA activity of AKAP121 contributes to the enhanced resistance of HT22-R against oxidative stress induced by exposure to excess glutamate. To address this hypothesis, we transiently transfected HT22-R cells with wild-type or PKA-binding deficient mutant of AKAP121 (AKAP121- Δ PKA) in its baseline culture medium containing 10 mM glutamate. We observed that cells transiently expressing AKAP121- Δ PKA showed significantly reduced mitochondrial interconnectivity and reduced mitochondrial content compared to HT22-R cells transfected with wild-type AKAP121 under baseline conditions (Fig. S2A–C). Interestingly, transient expression of AKAP121- Δ PKA significantly reduced cell viability in HT22-R cells treated with excess glutamate compared to cells transiently expressing OMM-GFP or wild-type AKAP121 (Fig. S2D). Overall, our data suggest that AKAP121- Δ PKA ablates the resistance of HT22-R cells against oxidative glutamate toxicity by acting in a dominant negative manner, presumably by outcompeting the

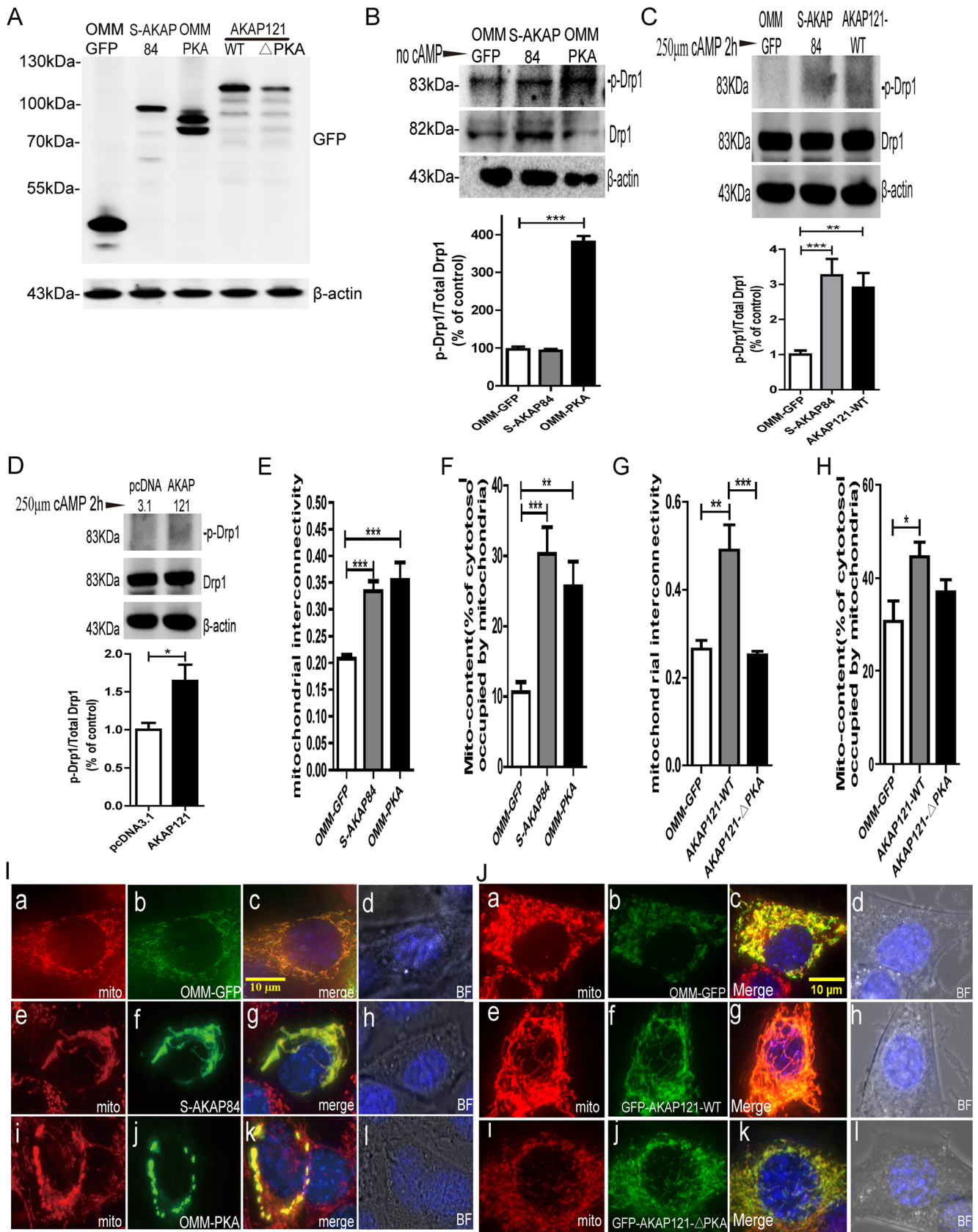


Fig. 4 Mitochondrial localized PKA promotes neuroprotection against glutamate oxidative toxicity by remodeling mitochondria and phosphorylating Drp1. **a** Lysates derived from cells transiently transfected the indicated plasmids were immunoblotted for GFP in order to analyze the expression level of vectors. The representative Western blot shows that transient expression level of the indicated vectors were detectable and expressed at the expected molecular weights for each recombinant protein as published [1]. **b** Lysates derived from HT22 transfected with OMM-GFP, S-AKAP84, and OMM-PKA were immunoblotted for p-Drp1 and total Drp1(T-Drp1) to analyze the ability of PKA-modulating plasmids to phosphorylate the AKAP121/PKA substrate Drp1 under basal conditions ($***p < 0.001$ vs. OMM-GFP, one-way ANOVA, Tukey's test). **c** Lysates derived from HT22 transfected with OMM-GFP, S-AKAP84, and AKAP121-WT were immunoblotted for p-Drp1 and total Drp1(T-Drp1) to analyze the ability of PKA-modulating plasmids to phosphorylate the AKAP121/PKA substrate Drp1 in the presence of 250 μ M cAMP for 2 h ($**p < 0.01$, $***p < 0.001$ vs. OMM-GFP, one-way ANOVA, Tukey's test). **d** Lysates derived from HT22 transfected with pcDNA3.1 and the full-length AKAP121 were immunoblotted for p-Drp1 and total Drp1 (T-Drp1) to analyze the ability of PKA-modulating plasmids to phosphorylate the AKAP121/PKA substrate Drp1 in the presence of 250 μ M cAMP for 2 h ($*p < 0.05$ vs. pcDNA3.1, Student's *t* test). **e** Image-based quantification of mitochondrial interconnectivity (area/perimeter ratio of mitochondrion per cell) in HT22 cells transiently transfected with the indicated PKA-modulating plasmids (for both graphs: $***p < 0.001$ vs. OMM-GFP, one-way ANOVA, Tukey's test). **f** Image-based quantification of mitochondrial content (% of cytosol occupied by mitochondria) in HT22 cells transiently transfected with the indicated PKA-modulating plasmids (for both graphs: $**p < 0.01$, $***p < 0.001$ vs. OMM-GFP, one-way ANOVA, Tukey's test). **g** Image-based quantification of mitochondrial interconnectivity (area/perimeter ratio of mitochondrion per cell) in HT22 cells transiently transfected with the indicated PKA-modulating plasmids (for both graphs: $**p < 0.01$, $***p < 0.001$ vs. OMM-GFP, one-way ANOVA, Tukey's test). **h** Quantification of mitochondrial content in HT22 cells transiently transfected with the indicated PKA-modulating plasmids (for both graphs: $*p < 0.05$ vs. OMM-GFP, one-way ANOVA, Tukey's test). **i** Representative immunofluorescent images of HT22 cells transfected with OMM-GFP, S-AKAP84, or OMM-PKA that were stained with 30 nm MitoTracker Red and 2 μ g/ml Hoechst 33342 for 15 min at 37 °C to visualize the mitochondria and nuclei respectively. RGB images were then captured through the midplane of the soma of cells by employing the API *DeltaVision Elite Live cell Imaging System* ((a, e, i) MitoTracker Red; (b, f, j) EGFP; (c, g, k) merged image of three colors; (d, h, l) Hoechst33342 with bright-field reference), scale bar = 10 μ m. **j** Representative immunofluorescent images of HT22 cells transfected with OMM-GFP, AKAP121-WT, and AKAP121- Δ PKA were stained with 30 nm MitoTracker Red and 2 μ g/ml Hoechst 33342 for 15 min at 37 °C to visualize the mitochondria and nuclei respectively. RGB images were captured through the midplane of the soma by employing the API *DeltaVision Elite Live cell Imaging System* ((a, e, i) MitoTracker Red; (b, f, j) EGFP; (c, g, k) merged image of three colors; (d, h, l) Hoechst33342 with bright-field reference), Scale bar = 10 μ m. All the data were pooled from experiments that were repeated at least three times which yielded similar results (a representative data set is shown)

endogenous catalytic of PKA from binding to AKAP121 in the mitochondrion as previously published [15, 16].

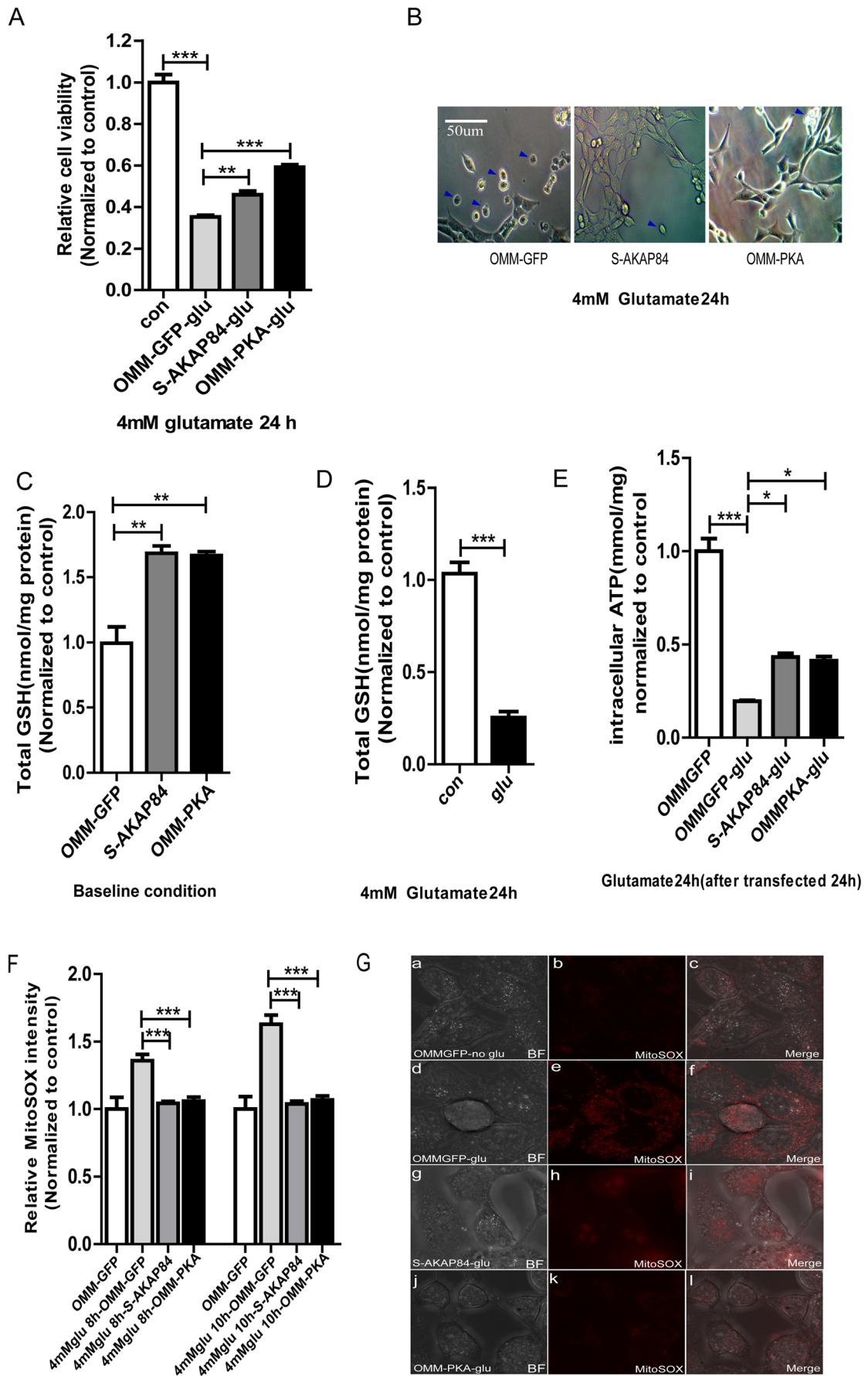
In aggregate, our data suggests that AKAP121 levels are increased in HT22 cells continuously exposed to excess glutamate as a compensatory response to reduce cell death induced by oxidative glutamate toxicity in HT22 cells.

Mechanistically, AKAP121/PKA-mediated phosphorylation of Drp1 contributes to enhanced neuronal survival against oxidative stress induced by oxidative glutamate toxicity in parental and in glutamate-resistant HT22 cells.

Discussion

Under physiological conditions, the cellular energy demands are predominantly met by ATP generated via oxidative phosphorylation in the mitochondrion. In particular, neurons are post-mitotic cells that heavily rely on high-quality mitochondria for the provision of energy required for the maintenance of neuronal connections and survival [14]. On the other hand, mitochondrial ROS are predominantly generated due to an inefficient electron flow from complex I to complex II in the inner mitochondrial membrane and matrix compartments, leading to the reduction of oxygen to superoxide. In particular, the production of mitochondrially localized ROS is significantly enhanced in conditions that produce oxidative stress in normoxic environments [6, 24]. Therefore, conditions that induce high and persistent levels of oxidative stress can rapidly damage mitochondria, shut down oxidative phosphorylation, and lead to a depletion of mitochondrial ATP levels, decreased mitochondrial biogenesis and turnover, and a high generation of mitochondrial superoxide, a precursor for the generation of other free radical species including hydroxyl radicals and peroxynitrites. To this end, exposing neurons to a high concentration of glutamate can overwhelm the cysteine/glutamate antiporter, leading to an excess intake of glutamate and an induction of high levels of oxidative stress due to a rapid and robust depletion of the antioxidant glutathione [6, 32, 35].

In this study, undifferentiated hippocampal progenitor HT22 neuronal cells, which do not express glutamate receptors, are highly vulnerable to glutamate-mediated toxicity due to oxidative stress caused via rapid extrusion of cysteine—a precursor amino acid required for the production of the antioxidant glutathione—through the activation of the cysteine/glutamate antiporter. The exposure of neuronal cells to excess exogenous glutamate caused robust mitochondrial pathology. Indeed, the acute exposure of HT22 neuronal cells to high concentrations of glutamate (~4 mM) leads to mitochondrial fission, increased production of mitochondrial superoxide, a massive depletion of ATP levels (~80% reduction) (Fig. 2), a depletion of glutathione levels (Fig. 2), a reduction of mitochondrial content, and the activation of apoptosis/cell death (Figs. 2d, 6g, h, and S3). However, it has been reported that either reversing the depletion of the cellular GSH content or overexpressing human SOD2 is sufficient to enhance cell survival of HT22 cells exposed to high concentration of glutamate [6, 19, 25, 32]. This observation underscores the importance of supplementing neurons with antioxidants to



◀ **Fig. 5** Mitochondrial localized PKA increases total GSH, reduced mitochondrial ROS and elevates neuronal survival against oxidative glutamate toxicity. **a** Overexpression of S-AKAP84 or OMM-PKA can protect neuronal HT22 cells from oxidative glutamate toxicity. Cells were transfected for 24 h and seeded in a 96-well culture plate at 5000 cells/well, overnight, and exposed to glutamate for 24 h. Cell viability was determined using the CCK-8 assay (for both graphs: $**p < 0.01$, $***p < 0.001$ vs. control, one-way ANOVA, Tukey's test). **b** Representative bright-field images of HT22 transfected with indicated vectors and incubated 4 mM glutamate for 24 h as analyzed by capturing phase-contrast images with a phase-contrast microscope. It is worth noting that cells transiently expressing S-AKAP84 or OMM-PKA and treated with glutamate exhibited a healthier cell morphology and less number of apoptotic or floating cells compared to cells transfected with an empty vector in the presence of glutamate. Scale bar = 50 μm . **c, d** Total glutathione content was measured in HT22 cells transiently transfected with the indicated plasmids under baseline conditions normalized to protein concentration (for the graphs: $**p < 0.01$, $***p < 0.001$ vs. OMM-GFP, one-way ANOVA; **c** Tukey's test, **d** Student's *t* test). **e** Total intracellular ATP content (μM ATP per μg of protein) was measured in HT22 cells transiently transfected with the indicated plasmids for 24 h in the presence or absence of 4 mM glutamate for another 24 h ($***p < 0.001$ vs. con, one-way ANOVA, Tukey's test). **f** Transfected HT22 cells were exposed to 4 mM glutamate for the indicated time points and stained with 5 μM MitoSOX Red to analyze for the level of mitochondrial superoxide. The bar graphs show the compiled quantification of the mean fluorescence intensity of MitoSOX in glutamate-treated HT22 cells as assessed by employing a fluorescence microplate reader and normalized to cell number measured by CCK-8 ($***p < 0.001$ vs. OMM-GFP, one-way ANOVA, Tukey's test). **g** Transfected HT22 cells were exposed to 4 mM glutamate for the indicated time point and stained with 5 μM MitoSOX Red, then subjected to immunofluorescence microscope. All the data were pooled from experiments that were repeated at least three times which yielded similar results (a representative data set is shown)

overcome the deleterious effects of oxidative stress induced by oxidative glutamate toxicity.

D-AKAP1 (AKAP140/149 and other splice variants AKAP121, S-AKAP84) is a protein scaffold that targets PKA to the outer mitochondrial membrane (OMM) to phosphorylate the pro-apoptotic protein BAD and the pro-fission protein Drp1 [13–15], a post-translational modification that leads to mitochondrial fusion and enhanced stability of mitochondrial networks. Therefore, an increase in PKA signaling in the mitochondrion via AKAP121 confers neuroprotection against a myriad of toxic insults that promote oxidative stress [8, 14, 16]. In addition, an elevation in PKA signaling in the mitochondrion via AKAP121 serves to regulate critical neuronal functions including mitochondrial dynamics, transport, function, turnover, and content in dendrites [15, 26, 36].

In this study, our data show for the first time that AKAP121 can confer neuroprotection in a neuronal model of glutamate oxidative toxicity. Transient expression techniques were used to determine whether the increased expression of endogenous AKAP121 observed in HT22 exposed to acute or chronic levels of glutamate (Fig. 2) contributes to neuroprotection. Indeed, transient expression of S-AKAP84, constitutively active mitochondrial PKA (OMM-PKA) or of AKAP121, but

not a PKA-binding deficient mutant version, is sufficient to enhance neuronal survival against oxidative glutamate toxicity (Figs. 2d, 5a, S2D, and E) suggesting that increased PKA signaling via AKAP121 in the mitochondrion is neuroprotective against oxidative glutamate toxicity. In response to increased mitochondrial PKA signaling, an increase in the mRNA and protein level of AKAP121 in the mitochondrion serves to elevate and “prime” antioxidant defense responses as a mechanism to enhance neuronal survival against glutamate oxidative toxicity in the HT22 hippocampal neuronal cell line.

Unexpectedly, our data show that overexpressing AKAP121 is detrimental during hypoxia as transient overexpression of AKAP121 significantly reduces cell viability in HT22 cells subjected to OGD/R (Fig. 2). It is conceivable that overexpression of AKAP121 enhances oxidative phosphorylation during OGD/R, leading to a detrimental increase in the production of mitochondrial ROS (superoxide) and subsequent cell death. Given that D-AKAP1 is rapidly targeted for proteolytic degradation via the E3 ligase Siah2 in a reductive environment caused by ischemia [31], it is also conceivable that PKA signaling in the mitochondrion is uncoupled via Siah2-mediated proteolytic degradation as a protective mechanism to attenuate any potential oxidative stress caused by a “burst” of oxidative phosphorylation activity that can ensue the reperfusion phase. Hence, our data suggest that the neuroprotective effects of AKAP121 require a normoxic environment.

Based on our data, we describe three molecular mechanisms by which enhanced PKA signaling confers neuroprotection against glutamate oxidative toxicity as elaborated below.

A Neuroprotective Feed-Forward Loop Is Activated by PKA in Response to Oxidative Stress

AKAP121 shows widespread expression in myriad of tissues. AKAP121 expression is transcriptionally regulated via the cAMP/PKA pathway in thyroid and testicular germ cells [29]. Other investigators further discovered that endogenous AKAP121 accumulates in neonatal ventricular myocytes in a cAMP-dependent manner as well [30].

The subcellular localization, as well as the strength and extent of increased PKA signaling are important for regulating critical neuronal functions and survival [14]. In neurons, several neurotrophic factors can engage cell surface receptors (e.g., tyrosine kinase receptors) to increase intracellular PKA signaling [37]. Hence, as consequence of increased cAMP signaling, the transcription factor CREB is phosphorylated by PKA in serine 133 to induce its nuclear translocation and subsequent activation of CREB-dependent transcription programs. Therefore, elevated CREB-mediated transcription leads to enhanced neuronal survival via an increase in transcription/translation of proteins that modulate neuronal

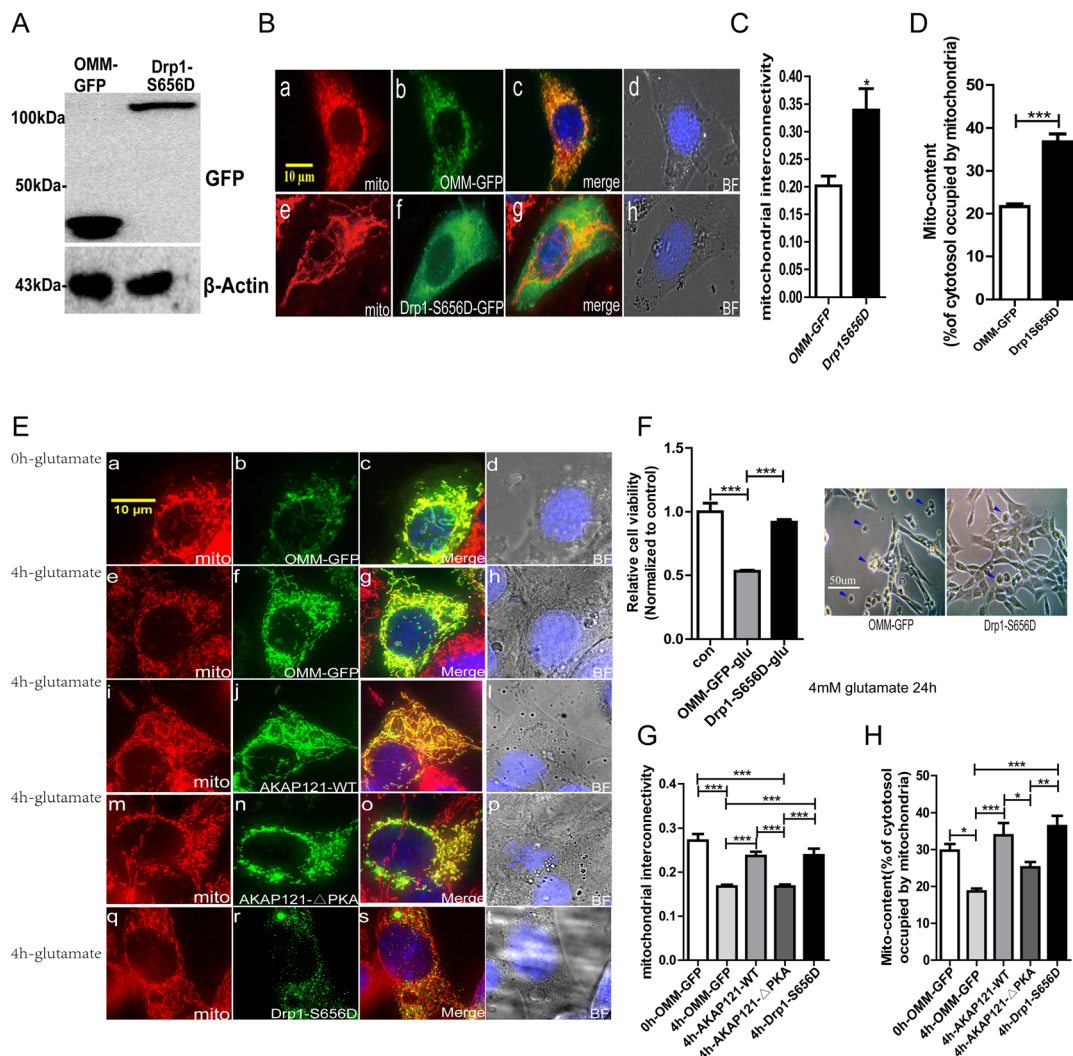


Fig. 6 The neuroprotective effects of AKAP121 are conferred via PKA-mediated phosphorylation of Drp1. **a** Lysates derived from cells transiently transfected with OMM-GFP control or with the PKA phosphomimetic of Drp1 (Drp1-Ser656Asp) were immunoblotted for GFP to analyze the levels of recombinant GFP-tagged proteins attained in HT22 cells under basal conditions. **b** HT22 cells were transfected with OMM-GFP control or with Drp1-S656D (Drp1-Ser656Asp) for 24 h. Cells were then stained with 30 nM MitoTracker Red and 2 μ g/ml Hoechst 33342 for 15 min at 37 $^{\circ}$ C to visualize the mitochondria and nuclei respectively under basal conditions. Fluorescent images were captured through the midplane of the soma by employing a *DeltaVision Elite Live cell Imaging System* ((a, e) MitoTracker Red; (b, f) EGFP; (c, g) merged image of three colors; (d, h) Hoechst33342 with bright-field reference), scale bar = 10 μ m. **c** Quantification of mitochondrial interconnectivity (area/perimeter ratio per cell) in HT22 cells transiently expressing Drp1-S656D or OMM-GFP control ($*p < 0.05$ vs. OMM-GFP, Student's *t* test). **d** Quantification of mitochondrial content (% of cytosol occupied by mitochondria) in HT22 cells transiently expressing Drp1-S656D vector or OMM-GFP control ($***p < 0.001$ vs. OMM-GFP, Student's *t* test). **e** HT22 cells were transfected with OMM-GFP control or with AKAP121-WT, AKAP121- Δ PKA, and Drp1-S656D for 24 h. Transfected HT22 cells were then subjected to 4 mM glutamate insults for 4 h and stained with 30 nM MitoTracker Red and 2 μ g/ml Hoechst 33342 for 15 min at 37 $^{\circ}$ C to visualize the mitochondria and nuclei respectively. Fluorescent images were captured through the midplane of the soma by employing a *DeltaVision Elite Live cell Imaging System* ((a,

e, i, m, q) MitoTracker Red; (b, f, j, n, r) EGFP; (c, g, k, o, s) merged image of three colors; (d, h, i, p, t) Hoechst33342 with bright-field reference), scale bar = 10 μ m. **f** Transient overexpression of Drp1-S656D significantly protects HT22 cells from glutamate toxicity. Cells were transfected for 24 h with the indicated plasmids and seeded in 96-well culture plates at 5000 cells/well overnight prior to exposing cells with 4 mM glutamate for 24 h. Cell viability was determined by employing the CCK-8 assay ($***p < 0.001$ vs. con, Student's *t* test). Right: the cell morphologies of cells exposed to glutamate were analyzed by capturing bright-field images by employing a phase-contrast microscope. Note that HT22 cells transiently expressing Drp1-S656D showed a healthier cell morphology, less number of floaters, and less number of apoptotic cells (condensed/shrunken) as indicated by blue arrowhead. Scale bar = 50 μ m. **g** Quantification of mitochondrial interconnectivity (area/perimeter ratio per cell) in HT22 cells transiently expressing AKAP121-WT, AKAP121- Δ PKA, Drp1-S656D, and OMM-GFP in the absence or presence of 4 h incubation of 4 mM glutamate ($***p < 0.001$, one-way ANOVA, Tukey's test). **h** Quantification of mitochondrial content (% of cytosol occupied by mitochondria) in HT22 cells transiently expressing AKAP121-WT, AKAP121- Δ PKA, Drp1-S656D, and OMM-GFP in the absence or presence of 4 h incubation of 4 mM glutamate incubation ($*p < 0.05$, $**p < 0.01$, $***p < 0.001$, one-way ANOVA, Tukey's test). All the data were pooled from experiments that were repeated at least three times which yielded similar results (a representative data set is shown)

survival, mitochondrial biogenesis/function, and cytoskeletal dynamics (e.g., Elk1, Bcl2) [38]. In this study, we report that increased intracellular level of cAMP level and phosphorylation CREB at Ser133 is pathologically induced by glutamate oxidative toxicity which leads to an increase in the protein levels of AKAP121 in the HT22 hippocampal progenitor neuronal cell line (Fig. 1). Therefore, our data suggest that oxidative stress induced by excess glutamate leads to a robust increase in endogenous cAMP levels signaling which leads to activation of PKA at the mitochondrion and cytosol, and leads to a feed-forward loop that serves to amplify PKA signaling in the mitochondrion by increasing the transcription and translation of endogenous AKAP121 (Fig. 1). Secondly, an increase in global cAMP-dependent signaling can lead to PKA-dependent phosphorylation of Drp1 to increase mitochondrial interconnectivity and thereby block apoptosis by phosphorylating the pro-fission modulator Drp1 and the pro-apoptotic protein BAD [8, 15, 16]. It is worth noting that our data show that increasing the fidelity of PKA signaling at the mitochondrion, by relocating endogenous PKA via AKAP121 (e.g., expressing AKAP121 or S-AKAP84), and that enhancing PKA signaling at the mitochondrion is sufficient to confer neuroprotection of HT22 cells against excess glutamate.

Our data suggests that PKA signaling is significantly up-regulated in both the mitochondrial and cytosolic compartments when neurons are chronically exposed to high concentrations of glutamate. As shown in our study, HT22 glutamate-resistant cells contained high levels of endogenous AKAP121 along with a concomitant increase in intracellular PKA signaling, as evident by increased cAMP-dependent activity and an elevated ratio of p-CREB to total CREB (Fig. 1). Given that treatment of HT22 cells with excess glutamate is associated with a robust time-dependent increase in global PKA signaling and PKA-mediated phosphorylation of CREB (Fig. 1), we cannot exclude the possibility that cytosolic/nuclear localized PKA also contributes to increase neuronal survival in our model of oxidative glutamate toxicity. Therefore, our data warrants future studies to analyze the extent to which cytosolic/nuclear PKA contributes to cytoprotection against glutamate-mediated oxidative stress.

AKAP121 Promotes Cytoprotection Against Glutamate Toxicity by Elevating Antioxidants Levels

As a second “line of defense,” we observed that increased D-AKAP121/PKA signaling enhances the levels of antioxidants GSH and of SOD2. GSH and SOD2 both play important roles in protecting cells against oxidative stress induced against a variety of toxic insults [6, 19, 25, 32]. In addition to tethering PKA/C to the OMM via type II regulatory subunits of PKA (PKA/RII β), D-AKAP1 increases the level of SOD2 mRNA to mitochondria to enhance SOD2 in a PKA activity-

dependent manner [18]. Consistent with this observation, our data shows that transient overexpression of AKAP121, which redirects the endogenous pool of PKA to mitochondria, or of OMM-PKA increases the mRNA and protein level of SOD2 mRNA in HT22 cells subjected to oxidative glutamate toxicity.

Consistent with our transient expression studies (Fig. 3c), our data showed that HT22-R cells also intrinsically show an elevated level of the antioxidants GSH and SOD2. In the presence of oxidative glutamate toxicity, it is conceivable that D-AKAP1/PKA increases the level of total GSH via an undescribed mechanism. However, previous studies have offered mechanistic insight into how glutamate oxidative toxicity increases GSH levels. For instance, glutamate-resistant HT22 cells have been shown to shuttle most of the available glucose towards the hexose monophosphate shunt in order to increase the recovery of total GSH [24]. HT22-R cells, which contain high level of D-AKAP1, may also resist glutamate oxidative toxicity via enhanced mitochondrial interconnectivity and mitochondrial content, leading to enhanced calcium loading by mitochondria and thereby blocking Drp1-dependent apoptosis. Our results suggest that enhancing PKA signaling, via transient expression of AKAP121 or S-AKAP84, elevates total GSH and reverses the depletion of ATP levels, cytoprotective events that are associated with increase resistance of neuronal cells to oxidative glutamate toxicity. However, the precise molecular mechanisms by which glutamate oxidative toxicity increases antioxidant defense mechanisms and undergoes metabolic switching to increase neuronal survival needs to be elucidated in future studies.

Another mechanism by which HT22 neuronal cells resist oxidative glutamate toxicity is via metabolic switching. Interestingly, HT22 glutamate-resistant cells have been reported to be resistant to inhibition of ATP synthesis when exposed to oligomycin, an inhibitor of the ATP synthase, suggesting that glutamate-resistant HT22 cells have the potential to undergo metabolic switching (reprogramming) to enhance glycolysis as compensatory mechanism to enhance resistance against oxidative stress induced by oxidative glutamate toxicity [24].

AKAP121/PKA Confers Neuroprotection Against Glutamate Toxicity via Mitochondrial Fusion

Drp1—a cytosolic dynamin GTPase—is post-translationally regulated by different ser/thr kinases and phosphatases, and unopposed Drp1 activity modulates not only mitochondrial shape and dynamics but also cell survival [34]. For instance, PKA-mediated phosphorylation of rat Drp1 at Ser656 induces mitochondrial elongation and resistance to apoptosis. Indeed, a PKA phosphomimetic mutant of Drp1 (Ser656D) robustly phenocopies many protective features of mitochondrial localized PKA in our neuronal model of oxidative glutamate

toxicity including enhancing mitochondrial interconnectivity, increasing mitochondrial content and enhancing mitochondrial health and oxidative phosphorylation (Figs. 4 and 6) [8, 20, 34]. However, we observed significant differences in how transient expression of Drp1-S656D or of OMM-PKA modulates mitochondrial morphology and content. For instance, following 24 h transfection, we observed that transient expression of OMM-PKA elicits a perinuclear clustering of mitochondria compared HT22 cells expressing Drp1-S656D (Figs. 4i and 6b, e). Although transient expression of S-AKAP84, AKAP121, OMM-PKA, or of Drp1-S656D increases mitochondrial interconnectivity and content per cell (Fig. 6), the molecular mechanisms by which increased D-AKAP121/PKA signaling elevate mitochondrial levels during oxidative glutamate toxicity need to be elucidated.

Conceptual Model and Future Directions

Thus far, our data suggest that chronic exposure to oxidative stress induced by exogenous glutamate leads to a well-orchestrated and steadfast upregulation of compensatory global PKA signaling to enhance AKAP121 levels. An increase in PKA signaling in the mitochondrion via AKAP121 leads to increased mitochondrial fusion and increased mitochondrial content and health by phosphorylating the pro-fission modulator Drp1 and by enhancing the mRNA/protein levels of SOD2 and GSH (Fig. 7). Up to this point, the molecular mechanisms by which glutamate oxidative toxicity activates PKA signaling should be addressed in a future study. For instance, it is conceivable that ser/thr phosphatases that oppose PKA signaling undergo ROS-mediated inactivation (thiol groups in critical cysteine residues are oxidized) as a result of the high accumulation of ROS caused by glutamate-mediated oxidative stress. In addition, it is conceivable that the activity of adenylate cyclases is elevated to increase cAMP levels via an undefined molecular mechanism. Hence, our data warrants future studies to resolve any remaining conceptual gaps in our conceptual model.

Therapeutic Implications of our Study

Given that AKAP121 can accumulate in during glutamate oxidative toxicity in a time-dependent and in a PKA activity-dependent manner (Fig. 1), our transient overexpression data suggest that the increased levels of endogenous AKAP121, which is induced by exposure to excess glutamate, is causally linked to enhanced mitochondrial health and function and increased resistance to oxidative stress. Therefore, acute oxidative stress can elicit a compensatory, neuroprotective signaling in HT22 cells. Conversely, pathological conditions that induce chronic stress can adversely shut down PKA signaling in the mitochondrion. For instance, in cardiac myocytes, one study showed that the level of signaling

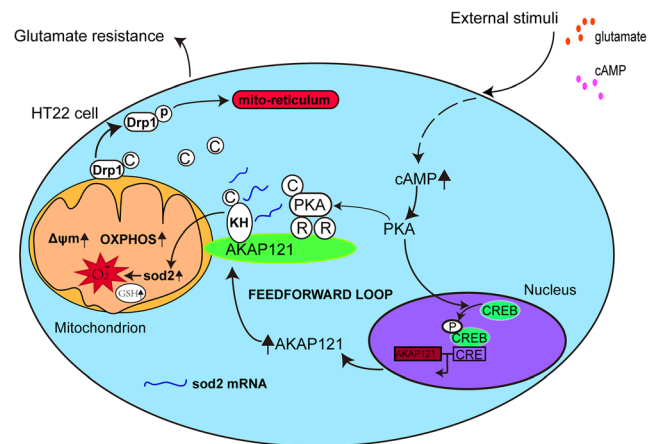


Fig. 7 The neuroprotective mechanisms of AKAP121/PKA in the cell culture model of oxidative glutamate toxicity. In HT22 cells, external stimuli or toxicity as induced by exposures to 4 mM glutamate, 10 mM glutamate chronic exposure, or to treatment with 250 μ M of exogenous cAMP can lead to an intracellular elevation of cAMP. The increase in the intracellular level of cAMP level activates PKA, which leads to PKA-mediated phosphorylation of CREB and thereby eliciting a transcriptional-mediated upregulation of the level of AKAP121. AKAP121 is targeted to the OMM to increase the amount and specificity of PKA at the mitochondrion. In this manner, AKAP121 facilitates PKA-cAMP signaling at the mitochondrion, enhances oxidative phosphorylation, and elevates $\Delta\psi_m$. Furthermore, cAMP, AKAP121, and mitochondrial PKA form a positive feed-forward loop which can enhance the strength and fidelity of PKA at the mitochondrion. Therefore, this feed-forward loop leads to enhanced survival of HT22 neuronal cells against oxidative glutamate toxicity via two mechanisms. First of all, mitochondrial PKA (AKAP121/PKA) can increase the rate of phosphorylation of Drp1, leading to the inactivation of this mechanoenzyme and to enhanced mitochondrial fusion to form interconnected mitochondrial networks. Hence, this elevated state of mitochondrial fusion confers neuroprotection against oxidative glutamate toxicity. Secondly, mitochondrial PKA can enhance the binding of SOD2 mRNA to the KH domain of AKAP121, leading to an increase in the level of mitochondrial SOD2. In addition, increased level of AKAP121 is associated with an increase in the level of total GSH through an unknown mechanism. Overall, elevated PKA signaling at the mitochondrion and at the cytosolic/nuclear compartments induced by oxidative glutamate toxicity elicits compensatory signaling pathways that serve to increase the level of antioxidants in the mitochondrion and increases mitochondrial health to confer increased resistance of HT22 cells against oxidative stress

regulated by the cAMP-p-CREB-AKAP121 molecular axis decreased progressively during pressure overload-induced by cardiac hypertrophy, molecular pathology that was associated with downregulation of endogenous AKAP121, increased ROS generation, and increased cell death [30].

Pharmacological approaches that can enhance the level of intracellular cAMP to increase protective PKA signaling at the mitochondrion via D-AKAP1 [29, 39] may represent a therapeutic strategy for treating several neurodegenerative disorders characterized by overt oxidative stress. Unfortunately, there are no pharmacological compounds that can exclusively stimulate D-AKAP1/PKA signaling in the mitochondrion. Therefore, in this context, D-AKAP1 represents an attractive

molecular target for treating neurodegenerative diseases characterized by overt oxidative stress, mitochondrial fission and mitochondrial dysfunction.

Conclusion

Besides increasing mitochondrial interconnectivity, we discovered that mitochondrial remodeling via mitochondrial PKA (AKAP121/PKA) blocks mitochondrial ROS production by upregulating mitochondrial and cytosolic antioxidant defense responses (e.g., increased levels of GSH and SOD2). Overall, our data shows that increased transcription and protein level of D-AKAP1 is governed via the cAMP-PKA-CREB signaling axis in neuronal cells subjected to oxidative glutamate toxicity as a protective mechanism to stabilize mitochondrial networks and function, reduce oxidative stress, and block cell death. Interestingly, increased mitochondrial PKA signaling required a normoxic but not a hypoxic environment to confer cytoprotection. Overall, our conceptual model suggests that D-AKAP1 plays a critical role in remodeling mitochondrial networks and conferring neuroprotection in neurons subjected to chronic oxidative stress that occurs in neurodegenerative diseases characterized by mitochondrial dysfunction (mitochondrial fission, loss of mitochondria, and ensued loss of oxidative phosphorylation) including Alzheimer's disease and Parkinson's disease.

Acknowledgments We thank Dr. Antonio Feliciello (Department of Molecular Medicine & Medical Biotechnology, University of Naples, Naples, Italy), Xingshun Xu (Institute of Neuroscience, Soochow University, China), Steven Green (Biology Department, University of Iowa, IA, USA), and Stefan Strack (Department of Pharmacology, University of Iowa Carver College of Medicine, IA, USA) for providing vectors and the HT22 cell line. We apologize to all colleagues whose important contributions to this field could not be cited due to space limitations.

Availability of Data and Materials The raw data files used and/or analyzed during the current study are available from the corresponding author on reasonable request.

Authors' Contributions Conceptualization and design of the study: Jingdian Zhang, Ming Zhang, Dagda RK, and Ying Zhang; methodology and investigation: Jingdian Zhang, Dagda RK, Feng Wang, Yumeng Wang, Xu Wang, Di Ma, Xiang Yin, Chunxiao Li; providing important research resources, materials, and scientific input: Jiachun Feng, Dagda RK, Ming Zhang, and Ying Zhang; writing the original manuscript draft: Jingdian Zhang and Dagda RK; review and editing: all authors; supervision: Ming Zhang, Dagda RK, Jiachun Feng, and Ying Zhang. All authors read and approved the final manuscript.

Funding This work was supported by the Natural Science Foundation of Jilin Province Science and Technology Development Plan (No. 20180101154JC) (to Ying Zhang), by NIH grants 1R01NS105783-01 and GM103554 (to Ruben K. Dagda), National Natural Science Foundation of China (No. 81771257) (to Jiachun Feng), and National

Natural Science Foundation for Young Scientists of China (No. 81701158) (to Di Ma).

Compliance with Ethical Standards

Ethics Approval and Consent to Participate Not applicable.

Consent for Publication Not applicable.

Competing Interests The authors declare that they have no competing interests.

Publisher's Note Springer Nature remains neutral with regard to jurisdictional claims in published maps and institutional affiliations.

References

- Coyle JT, Puttfarcken P (1993) Oxidative stress, glutamate, and neurodegenerative disorders. *Science* 262(5134):689–695
- Gardoni F, Di Luca M (2015) Targeting glutamatergic synapses in Parkinson's disease. *Curr Opin Pharmacol* 20:24–28
- Dong XX, Wang Y, Qin ZH (2009) Molecular mechanisms of excitotoxicity and their relevance to pathogenesis of neurodegenerative diseases. *Acta Pharmacol Sin* 30:379–387
- Murphy TH, Miyamoto M, Sastre A, Schnaar RL, Coyle JT (1989) Glutamate toxicity in a neuronal cell line involves inhibition of cystine transport leading to oxidative stress. *Neuron* 2:1547–1558
- Fukui M, Song JH, Choi J, Choi HJ, Zhu BT (2009) Mechanism of glutamate-induced neurotoxicity in HT22 mouse hippocampal cells. *Eur J Pharmacol* 617:1–11
- Fukui M, Zhu BT (2010) Mitochondrial superoxide dismutase SOD2, but not cytosolic SOD1, plays a critical role in protection against glutamate-induced oxidative stress and cell death in HT22 neuronal cells. *Free Radic Biol Med* 48:821–830
- Maher P, Davis JB (1996) The role of monoamine metabolism in oxidative glutamate toxicity. *J Neurosci* 16:6394–6401
- Merrill RA, Dagda RK, Dickey AS, Cribbs JT, Green SH, Usachev YM, Strack S (2011) Mechanism of neuroprotective mitochondrial remodeling by PKA/AKAP1. *PLoS Biol* 9:e1000612
- Flippo KH, Strack S (2017) Mitochondrial dynamics in neuronal injury, development and plasticity. *J Cell Sci* 130:671–681
- Wasilewski M, Scorrano L (2009) The changing shape of mitochondrial apoptosis. *Trends Endocrinol Metab* 20:287–294
- Chen H, Chan DC (2009) Mitochondrial dynamics-fusion, fission, movement, and mitophagy-in neurodegenerative diseases. *Hum Mol Genet* 18:R169–R176
- Grohm J, Kim SW, Mamrak U, Tobaben S, Cassidy-Stone A, Nunnari J, Plesnila N, Culmsee C (2012) Inhibition of Drp1 provides neuroprotection in vitro and in vivo. *Cell Death Differ* 19:1446–1458
- Merrill RA, Strack S (2014) Mitochondria: A kinase anchoring protein 1, a signaling platform for mitochondrial form and function. *Int J Biochem Cell Biol* 48:92–96
- Dagda RK, Das Banerjee T (2015) Role of protein kinase A in regulating mitochondrial function and neuronal development: implications to neurodegenerative diseases. *Rev Neurosci* 26:359–370
- Affaitati A, Cardone L, de Cristofaro T, Carlucci A, Ginsberg MD, Varrone S, Gottesman ME, Avvedimento EV et al (2003) Essential role of A-kinase anchor protein 121 for cAMP signaling to mitochondria. *J Biol Chem* 278:4286–4294
- Dagda RK, Gusdon AM, Pien I, Strack S, Green S, Li C, Van Houten B, Cherra SJ 3rd et al (2011) Mitochondrially localized

- PKA reverses mitochondrial pathology and dysfunction in a cellular model of Parkinson's disease. *Cell Death Differ* 18:1914–1923
17. DasBanerjee T, Dagda RY, Dagda M, Chu CT, Rice M, Vazquez-Mayorga E, Dagda RK (2017) PINK1 regulates mitochondrial trafficking in dendrites of cortical neurons through mitochondrial PKA. *J Neurochem* 142:545–559
 18. Ginsberg MD, Feliciello A, Jones JK, Avvedimento EV, Gottesman ME (2003) PKA-dependent binding of mRNA to the mitochondrial AKAP121 protein. *J Mol Biol* 327:885–897
 19. Sahin M, Saxena A, Joost P, Lewerenz J, Methner A (2006) Induction of Bcl-2 by functional regulation of G-protein coupled receptors protects from oxidative glutamate toxicity by increasing glutathione. *Free Radic Res* 40:1113–1123
 20. Cribbs JT, Strack S (2007) Reversible phosphorylation of Drp1 by cyclic AMP-dependent protein kinase and calcineurin regulates mitochondrial fission and cell death. *EMBO Rep* 8:939–944
 21. Wang W, Zhao L, Bai F, Zhang T, Dong H, Liu L (2016) The protective effect of dopamine against OGD/R injury-induced cell death in HT22 mouse hippocampal cells. *Environ Toxicol Pharmacol* 42:176–182
 22. Dagda RK, Cherra SJ 3rd, Kulich SM, Tandon A, Park D, Chu CT (2009) Loss of PINK1 function promotes mitophagy through effects on oxidative stress and mitochondrial fission. *J Biol Chem* 284:13843–13855
 23. Sheng B, Gong K, Niu Y, Liu L, Yan Y, Lu G, Zhang L, Hu M et al (2009) Inhibition of gamma-secretase activity reduces Abeta production, reduces oxidative stress, increases mitochondrial activity and leads to reduced vulnerability to apoptosis: implications for the treatment of Alzheimer's disease. *Free Radic Biol Med* 46:1362–1375
 24. Pfeiffer A, Pouya A, Jaeckel M, Schacht T, Schweiger S, Lewerenz J, Schäfer MKE, Noack R et al (2014) Mitochondrial function and energy metabolism in neuronal HT22 cells resistant to oxidative stress. *Br J Pharmacol* 171:2147–2158
 25. Lewerenz J, Letz J, Methner A (2003) Activation of stimulatory heterotrimeric G proteins increases glutathione and protects neuronal cells against oxidative stress. *J Neurochem* 87:522–531
 26. Bok J, Zha X-M, Cho Y-S, Green a SH (2003) An extranuclear locus of cAMP-dependent protein kinase action is necessary and sufficient for promotion of spiral ganglion neuronal survival by cAMP. *J Neurosci* 23(3):777–787
 27. Hu Y, Pan S, Zhang HT (2017) Interaction of Cdk5 and cAMP/PKA signaling in the mediation of neuropsychiatric and neurodegenerative diseases. *Adv Neurobiol* 17:45–61
 28. Kanga Pride C, Mo L, Quesnelle K, Dagda RK, Murillo D, Geary L, Corey C, Portella R et al (2014) Nitrite activates protein kinase A in normoxia to mediate mitochondrial fusion and tolerance to ischaemia/reperfusion. *Cardiovasc Res* 101:57–68
 29. Feliciello A, Rubin CS, Avvedimento EV, Gottesman a ME (1998) Expression of A kinase anchor protein 121 is regulated by hormones in thyroid and testicular germ cells. *J Biol Chem* 273:23361–23366
 30. Perrino C, Feliciello A, Schiattarella GG, Esposito G, Guerriero R, Zaccaro L, Del Gatto A, Saviano M et al (2010) AKAP121 down-regulation impairs protective cAMP signals, promotes mitochondrial dysfunction, and increases oxidative stress. *Cardiovasc Res* 88:101–110
 31. Carlucci A, Adornetto A, Scorziello A, Viggiano D, Foca M, Cuomo O, Annunziato L, Gottesman M et al (2008) Proteolysis of AKAP121 regulates mitochondrial activity during cellular hypoxia and brain ischaemia. *EMBO J* 27:1073–1084
 32. Fukui M, Choi HJ, Zhu BT (2010) Mechanism for the protective effect of resveratrol against oxidative stress-induced neuronal death. *Free Radic Biol Med* 49:800–813
 33. Ma Y, Taylor SS (2008) A molecular switch for targeting between endoplasmic reticulum (ER) and mitochondria: conversion of a mitochondria-targeting element into an ER-targeting signal in DAKAP1. *J Biol Chem* 283:11743–11751
 34. Jahani-Asl A, Slack RS (2007) The phosphorylation state of Drp1 determines cell fate. *EMBO Rep* 8:912–913
 35. Lewerenz J, Klein M, Methner A (2006) Cooperative action of glutamate transporters and cystine/glutamate antiporter system Xc- protects from oxidative glutamate toxicity. *J Neurochem* 98:916–925
 36. Carlucci A, Lignitto L, Feliciello A (2008) Control of mitochondria dynamics and oxidative metabolism by cAMP, AKAPs and the proteasome. *Trends Cell Biol* 18:604–613
 37. Kim HA, DeClue JE, Ratner N (1997) cAMP dependent protein kinase A is required for Schwann cell growth interactions between the cAMP and neuregulin tyrosine kinase pathways. *J Neurosci Res* 49:236–247
 38. Walton MR, Dragunow a M (2000) Is CREB a key to neuronal survival. *Trends Neurosci* 23:48–53
 39. Feliciello A, Gottesman ME, Avvedimento EV (2005) cAMP-PKA signaling to the mitochondria: protein scaffolds, mRNA and phosphatases. *Cell Signal* 17:279–287